TRIBHUVAN UNIVERSITY
INSTITUTE OF ENGINEERING
PULCHOWK CAMPUS

Thesis No: M-98-MSMDE-2024-2026

COUPLED LATERAL AND TORSIONAL VIBRATION ANALYSIS OF A ROTOR RUNNER SYSTEM WITH AN INTERNALLY SUPPORTED UNBALANCED RUNNER AND AN OVERHUNG BALANCED ROTOR

by

Bishal Kumar

A THESIS
SUBMITTED TO THE DEPARTMENT OF MECHANICAL AND AEROSPACE ENGINEERING IN PARTIAL FULFILLMENT OF THE REQUIREMENTS FOR THE DEGREE OF MASTER OF SCIENCE IN MECHANICAL SYSTEMS DESIGN AND ENGINEERING

DEPARTMENT OF MECHANICAL AND AEROSPACE ENGINEERING
LALITPUR, NEPAL

APRIL, 2026

COPYRIGHT

TRIBHUVAN UNIVERSITY
INSTITUTE OF ENGINEERING
PULCHOWK CAMPUS
DEPARTMENT OF MECHANICAL AND AEROSPACE ENGINEERING

The undersigned certify that they have read, and recommended to the Institute of Engineering for acceptance, a thesis entitled "**Coupled Lateral and Torsional Vibration Analysis of a Rotor Runner System With an Internally Supported Unbalanced Runner and an Overhung Balanced Rotor**" submitted by **Bishal Kumar** ***[CRN: PUL080MSMDE007]*** in partial fulfillment of the requirements for the degree of Master of Science in Mechanical Systems Design and Engineering.

Supervisor, Mahesh Chandra Luintel, Ph.D.
Professor
Department of Mechanical and Aerospace Engineering
Pulchowk Campus, Institute of Engineering, Lalitpur, Nepal

Supervisor, Surya Prasad Adhikari, Ph.D.
Professor
Department of Mechanical and Aerospace Engineering
Pulchowk Campus, Institute of Engineering, Lalitpur, Nepal

External Examiner, Er. Madhav Baral
Senior Mechanical Engineer
Hydro-Consult Engineering Ltd.
Buddhanagar, Kathmandu, Nepal

Tribhuvan University
Institute of Engineering
Department of Mechanical and Aerospace Engineering
Pulchowk Campus

Committee Chairperson, Sudip Bhattrai, Ph.D.
Assistant Professor and Head
Department of Mechanical and Aerospace Engineering
Pulchowk Campus, Institute of Engineering, Lalitpur, Nepal

Date: April 27, 2026 *[Baishakh 14, 2083]*

ABSTRACT

This study investigates the coupled lateral and torsional vibration analysis of a rotor-runner system comprising an internally supported unbalanced runner and an overhung balanced rotor. The Extended Hamilton's principle is employed on the Euler-Bernoulli beam model to obtain the governing differential equation of motion. To decouple the equation of motion for hierarchical separation of equations into different orders, a perturbation-based expansion approach is deployed, which assists in the investigation of the interaction between lateral and torsional vibrations. The resulting system of equations is solved using the assumed mode method to obtain the coupled torsional response of the given rotodynamic system. A numerical example implementation is done to validate the analytical solution, with the simulation results. At $x = \frac{L}{3}$, the analytical values are found to be 6.726 mm (0.027 rad) and 6.985 mm (0.028 rad) from simulation, while at $x = L$, the analytical results are found to be 13.453 mm (0.054 rad), and the simulation yielded 14.571 mm (0.058 rad).

ACKNOWLEDGEMENTS

I would like to express my sincere gratitude to all those who have supported and guided me during this thesis work. I am indebted to my Supervisors, Prof. Dr. Mahesh Chandra Luintel, whose belief and inspiration in my abilities have truly fueled this work, and to Prof. Dr. Surya Prasad Adhikari for his continuous motivation and guidance throughout every stage of this study. I would also like to extend my sincere thanks to Prof. Dr. Laxman Poudel for his continuous motivation throughout.

I would like to sincerely thank the Department of Mechanical and Aerospace Engineering, Pulchowk Campus, for their valuable guidance and academic support for this study. I also acknowledge the Department of Automobile and Mechanical Engineering, Thapathali Campus, Dr. Khem Gyanwali, Dr. Raj Kumar Chaulagain, Er. Debendra Bahadur Raut, Er. Bikki Chhantyal, Er. Bibek Dhungana and Dinanath Padhya for their consistent guidance and support.

Last but not least, I am ever grateful to my family members, Mr. Birendra Jha (Father), Mrs. Rina Kumari Jha (Mother), Mrs. Mansy Jha (Sister), and Ms. Shrisha Jha (Niece) for their unconditional support, patience, and encouragement at every step.

TABLE OF CONTENTS

LIST OF TABLES

LIST OF FIGURES

LIST OF ABBREVIATIONS

ODE	:	Ordinary Differential Equation
SDOF	:	Single Degree of Freedom

LIST OF SYMBOLS

ρ	:	Density of the shaft material
A	:	Area of cross-section of the shaft
ω	:	Angular velocity
Ω	:	Angular speed
G	:	Shear modulus of the shaft material
E	:	Young's Modulus of the shaft material
J	:	Area moment of inertia of the shaft
L	:	Length of the shaft
I_{PS}	:	Polar moment of inertia of the shaft
I_{DS}	:	Diametrical moment of inertia of the shaft
I_{PD1}	:	Polar moment of inertia of the first disc
I_{DD1}	:	Diametrical moment of inertia of the first disc
I_{PD2}	:	Polar moment of inertia of the second disc
I_{DD2}	:	Diametrical moment of inertia of the second disc
m	:	Mass per unit length of the shaft
M_{D1}	:	Mass of the first disc
M_{D2}	:	Mass of the second disc
e_s	:	Eccentricity in the shaft
β_s	:	Unbalanced phase in the shaft
e_D	:	Eccentricity in the disc

β_D	:	Unbalanced phase in the disc
u	:	Displacement in the direction of x
v	:	Displacement in the direction of y
w	:	Displacement in the direction of z
ψ	:	Euler angle rotation about z axis
θ	:	Euler angle rotation about y axis
ϕ	:	Euler angle rotation about x axis
T	:	Torque on the shaft
$F_{Shaft,y}$	:	Force in shaft in direction of y
$F_{Shaft,z}$	:	Force in shaft in direction of z
$F_{Disc,y}$	:	Force in disc in direction of y
$F_{Disc,y}$	:	Force in disc in direction of z
W_{nc}	:	Non conservative work

CHAPTER ONE: INTRODUCTION

1.1. Background

The necessity for in-depth analysis and research on rotating machinery has grown radically due to its increasing demand. Rotodynamic systems are frequently employed in contemporary industrial facilities and are essential to many different applications. One typical example of such systems is a pump. In addition to these, these types of systems are often expected to operate reliably under harsh and continuous service conditions. Even though the design conditons are greatly addressed, the interaction between lateral and torsional vibrations is one of the common causes of failure, which makes their study more crucial.

These systems have been extensively studied using various theoretical models since their dynamic response is of great importance. To better represent the real-world operating circumstances, such studies usually incorporate a wide range of assumptions and boundary conditions, along with the investigations of free and forced vibration.

A rotor-runner system generally consists of a rotating shaft (rotor) coupled to a runner, which essentially serves as an energy-conversion element in rotodynamic machines like turbines and pumps. In several configurations, the rotor extends overhanging or cantilevered while the runner is supported internally between bearings. This structural arrangement introduces an inherent asymmetric distribution of mass and stiffness in the system, making the overall vibration characteristics of the system much more complex in behaviour.

Furthermore, the runner can develop an imbalance due to fluid-structure interactions, wear, and manufacturing tolerances. Simplified uncoupled models are quite unable to accurately capture the coupled dynamic response of such systems caused by this imbalance, which is essentially transmitted through the shaft even where the rotor is balanced.

1.2. Problem statement

Most of the existing rotor dynamics research has primarily focused on symmetric configuration and uncoupled vibration modes often assuming balanced distribution of mass and stiffness. In particular, there has been limited research on rotor-runner systems in which the rotor is overhung beyond the last bearing support and the runner is unbalanced and supported internally between bearings. Traditional investigations, which usually treat lateral and torsional vibrations separately, fail to adequately capture the asymmetry in structure and dynamic complexities introduced by this configuration in particular.

The interaction between the unbalanced forces in the internally supported runner and the overhung geometry rotor leads to strong coupling in lateral as well as torsional behavior. Despite its practical significance in hydro-mechanical and turbomachinery systems, this coupled vibration phenomena has not been extensively explored. By creating a model that explicitly takes mass eccentricity and geometric asymmetry into account present in such rotodynamic systems, this study attempts to present insight on the coupled lateral and torsional vibrations in such systems.

1.3. Research objectives

1.3.1. Main objective

a) To develop a dynamic model and determine the coupled lateral and torsional vibration response of a rotor-runner system with an internally supported unbalanced runner and an overhung balanced rotor.

1.3.2. Specific objective

a) To develop the governing differential equation of motion using Extended Hamilton's principle for the Euler-Bernoulli beam model.
b) To make a hierarchical separation of the equation of motion into different orders using a perturbation series to study the extent of interaction.
c) To develop and formulate a transcendental mode shape function for a pinned-pinned overhung beam with a lumped mass at the free end and an intermediate lumped mass.
d) To solve the equation of motion for coupled vibration using the assumed mode method.
e) To perform a numerical example implementation on the solutions obtained and study the coupled torsional vibration.

1.4. Scope and assumptions of the study

This study is envisioned to study the coupled lateral and torsional forced vibrations of a rotor-runner system with a given fixed imbalance in the runner and an overhung balanced rotor, focusing on torsional vibration response relevant to hydro-mechanical pumps applications.

Following assumptions are taken for development and analysis of this model:

a) The runner and the rotor is assumed to be rigid.
b) Bearings are considered rigid with no deformation.
c) Longitudinal displacement of the shaft is neglected.

d) Damping effects in the bearings are ignored.

e) Torsional and flexural deformations are assumed to be of the same order.

f) Material damping variations are not considered.

CHAPTER TWO: LITERATURE REVIEW

2.1. Overview of the Rotodynamic system

Most of the rotodynamic systems comprise of a runner mounted (which is essentially an energy conversion element) on a shaft with a generator rotor positioned in an overhung configuration (as shown in **Figure 1**).

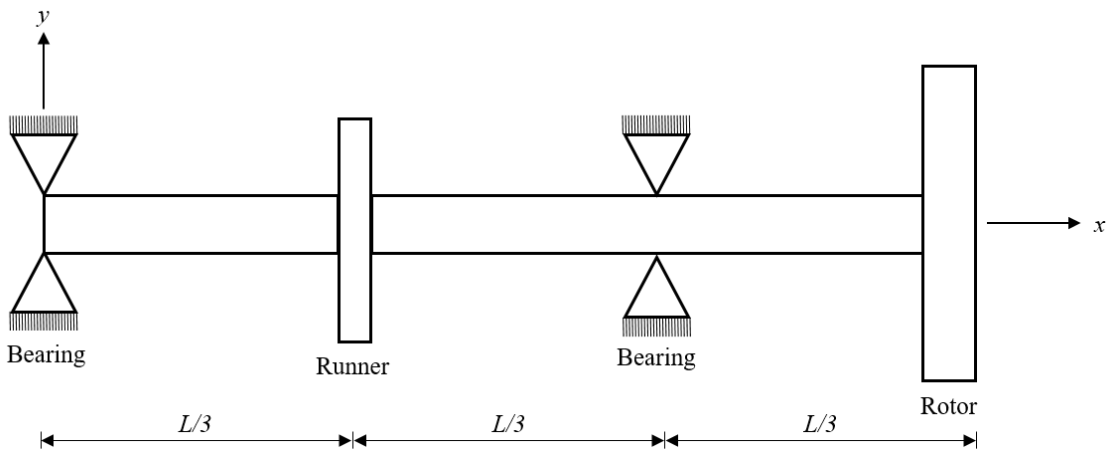

Figure 1: *A common rotodynamic system.*

2.2. Literature survey

The theoretical foundation for the study of dynamic stability in rotating systems was established on the grounds of fundamental issues in rotor dynamics. This is regarded as one of the first contributions to comprehending the intricate interactions of vibrational modes in rotor assemblies, particularly in association with the system on parametric excitation and the phenomenon of resonance (Tondl, 1965).

An analytical framework for comprehending the interaction between flexural and torsional modes in complex rotodynamic systems with continuous mass and stiffness distributions was established through the study of coupled flexural-torsional vibrations of rotors. This early work presented the importance of presenting continuous structural coupling and provided in-depth insights into the dynamic behaviour of rotors beyond simplified discrete mass approximations (Broniarek, 1968).

The dynamic behaviour of unbalanced rotors during acceleration through critical speeds was studied with a focus on the amplification of vibration amplitudes and transitory effects, examining how imbalance in mass influences response of rotor while passing through regions

of resonance. These findings presented the necessity of predicting precise critical operating speed and controlled acceleration tactics in unbalanced rotor systems (Gasch et al., 1979).

Seal ring-induced spiral vibrations in turbo-generators were studied in the context of rotating shafts for forced resonances, including flexural-torsional coupling. This work presented the importance of peripheral elements like seal rings in influencing rotor stability by showing how seal ring dynamics can interact with shaft flexure and torsion, producing complex resonance (Kellenberger, 1980).

The coupled torsional and transverse vibrations in unbalanced rotors were investigated using an analytical model, which highlighted that ignoring the interaction between flexural and torsional modes could lead to inaccurate predictions of critical speeds and vibration amplitudes. The study highlighted how important it is to take account of coupling effects in systems with large mass imbalance, in particular (Cohen & Porat, 1985).

The idea of bisynchronous torsional vibrations in rotating shafts introduced the concept that residual unbalance and synchronous whirling can produce torsional oscillations at twice the rotational frequency. The study showed how torsional modes can be excited in general by flexural motion effects even without any external torque stimulation (Bernasconi, 1987).

Both linear and nonlinear modelling were employed to investigate thecoupling between torsional and flexural deformations in the case of rotating shafts. The results revealed that the interaction between these two deformation modes has a significant impact on the rotor's dynamic response. The study clearly highlighted the necessity to account for torsion-bending coupling when analysing high-speed rotating machinery (Nataraj, 1993).

A dynamic model incorporating both shaft torsional and blade bending deformations in rotors highlighted the importance of including blade flexibility in rotor dynamics problem. The study presented that if coupled effects are not appropriately taken into account, they may potentially lead to dynamic instability (Al-Bedoor, 1999).

The coupled bending-torsional behaviour of rotors was investigated using the finite element model, which showed that taking both bending and torsional effects to the FEM model produced more accurate mode shapes and natural frequency values. In addition to these, this approach made it possible to evaluate sensitivity to structural flexibility in more precise manner (Mohiuddin & Khulief, 1999).

Both theoretical and experimental studies were employed to study coupled torsional-lateral vibrations in rotors. Numerical estimates were verified using experimental data, signifying that

ignoring coupling in vibration leads to differences between modelled and observed behaviour. The study reinforced the importance of taking coupling effects into account while solving rotating machinery faults (Perera, 1998).

The analysis of transient torsional and lateral vibrations of unbalanced rotors with rotor-to-stator rubbing was conducted to understand the interactions that lead to the introduction of non-linearities in the system response. The study presented that rubbing greatly increases vibration responsiveness and often leads to instability of rotors (Al-Bedoor, 2000).

Coupled torsional and lateral vibrations in unbalanced rotors under forced stimulation were investigated to study how unbalance and coupling impact critical speeds, response amplitudes, and overall dynamic behaviour. The results indicated that neglecting such factors can lead to an underestimation of vibrational severity (Al-Bedoor, 2001).

The investigation into bending-torsion coupling in rotor systems under rub-impact conditions indicated increased susceptibility to rubbing pressures and notable changes in frequency response and amplitude characteristics. The study emphasized how crucial it is to take coupling into account in contact-based rotor models (Zheng-ce et al., 2003).

The study of coupled bending, longitudinal, and torsional vibrations of a balanced rotor stressed that the internal coupling processes are sufficiently capable enough to produce complicated vibration patterns even in the absence of unbalance. (Darpe et al., 2004).

A stability study of spinning blade systems under torsional excitation showed that the torsional inputs can destabilise blade bending modes, particularly under conditions of resonance. This investigation enhanced knowledge regarding how torsional stresses influence the rotor stability and integrity of blades (Al-Bedoor & Al-Qaisia, 2005).

Using Hamilton's principle along with perturbation-based expansion, the coupled transverse and torsional vibration behaviour of a rigid disc mounted on a simply supported flexible shaft was studied. The study demonstrated that coupling effects are seen at second and higher orders. The study highlighted non-linear coupling effects in flexible shaft-disk systems leads to the observation of resonance when rotor speed approaches approximately half of the torsional natural frequency (Poudel & Luintel, 2022).

Similarly, an investigation on the torsional-flexural interaction in a shaft-disk system modelled as a rotating Euler-Bernoulli beam with a stiff disc highlighted that coupling appears in second-order equations only, not in first order. The analysis of a double overhung rotor demonstrated

that the higher-order effects are crucial for accurately representing torsional-lateral interaction in real-world rotating machines (Dahal et al., 2023).

Despite these studies, the analysis of coupled vibrations in rotodynamic systems with a pinned-pinned overhung structure exposed to torsional stimulation has received relatively little attention, out in the field of rotor dynamics. Hence, this study focuses on investigating coupled vibration analysis of such systems.

CHAPTER THREE: RESEARCH METHODOLOGY

This study is carried out using the following methodology.

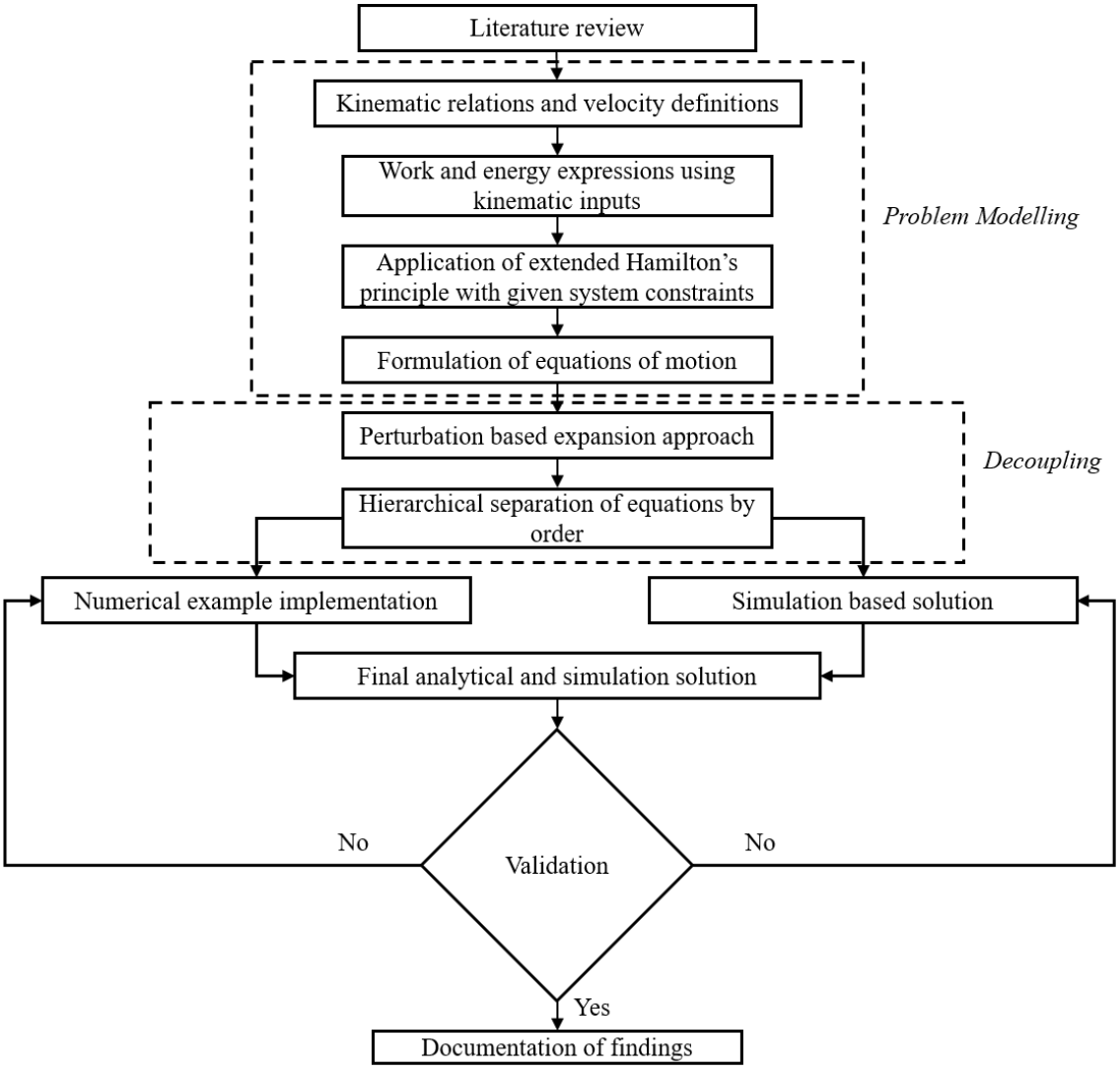

Figure 2: *Research methodology.*

The methodology begins with a Literature Review to institute a foundational understanding of the problem. This is trailed by a Problem Modelling phase, where the system is mathematically defined. This phase includes instituting kinematic relations, formulating work and energy expressions, and applying the extended Hamilton's principle with given system constraints to develop the governing equations of motion.

To simplify these complex governing differential equations, a decoupling phase is introduced, which deploys a perturbation-based expansion method. This leads to a hierarchical separation of the equations by order, making them easier and convenient to solve.

The methodology is then bifurcated into two parallel approaches: a Numerical example implementation and a simulation-based analysis. The results from both paths are amalgamated into a Final analytical and simulation solution.

A precarious Validation step follows, where the solution is checked. If the solutions fail to validate, the process rounds back to the implementation and simulation steps for enhancement. Upon successful validation, the final step is the Documentation of findings, which summarizes the results and conclusions of the entire process.

CHAPTER FOUR: MATHEMATICAL MODELLING

4.1. Kinematics of the system

4.1.1. Coordinate system

Let $OXYZ$ denote the fixed coordinate system, which is essentially treated as an inertial reference frame in this study. Similarly, let $oxyz$ represent the body fixed frame. When the systems of coordinate, namely, the inertial frame and the body fixed frame, are initially coincident, then the series of rotations (as shown in **Figure 3**) is performed in the sequence of ψ about z, θ about y, and ϕ about x, which is sufficient enough to achieve any arbitrary configuration of $oxyz$ coordinate system.

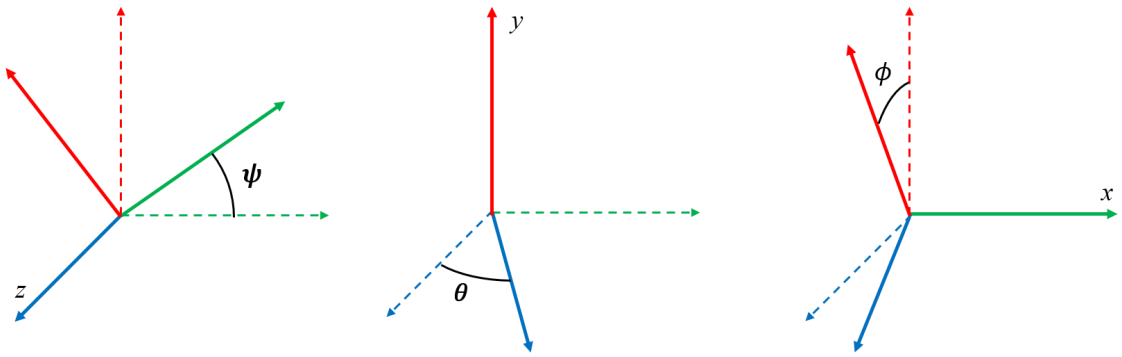

Figure 3: *Rotation sequence.*

The rotation matrix for ψ about z is given as shown in **Equation (1)**,

$$R_z(\psi) = \begin{bmatrix} \cos\psi & \sin\psi & 0 \\ -\sin\psi & \cos\psi & 0 \\ 0 & 0 & 1 \end{bmatrix} \quad (1)$$

The rotation matrix for θ about y is given as shown in **Equation (2)**,

$$R_y(\theta) = \begin{bmatrix} \cos\theta & 0 & -\sin\theta \\ 0 & 1 & 0 \\ \sin\theta & 0 & \cos\theta \end{bmatrix} \quad (2)$$

Similarly, the rotation matrix for ϕ about x is given as shown in **Equation (3)**,

$$R_y(\theta) = \begin{bmatrix} 1 & 0 & 0 \\ 0 & \cos\phi & \sin\phi \\ 0 & -\sin\phi & \cos\phi \end{bmatrix} \quad (3)$$

The final rotation matrix is given as shown in **Equation (4)**,

$$T = \begin{bmatrix} \cos\psi\cos\theta & \cos\theta\sin\psi & -\sin\theta \\ \sin\phi\sin\theta\cos\psi - \cos\phi\sin\psi & \sin\phi\sin\theta\sin\psi + \cos\phi\cos\psi & \sin\phi\cos\theta \\ \cos\phi\sin\theta\cos\psi + \sin\phi\sin\psi & \cos\phi\sin\theta\sin\psi - \sin\phi\cos\psi & \cos\phi\cos\theta \end{bmatrix} \quad (4)$$

4.1.2. Expression for velocity

The angular velocity of the system in the body fixed frame is given by the vector sum of time derivatives of Euler angles, as shown in **Equation (5)**.

$$\begin{bmatrix}\omega_x\\ \omega_y\\ \omega_z\end{bmatrix} = \begin{bmatrix}-\dot{\psi}sin\theta + \dot{\phi}\\ \dot{\theta}cos\phi + \dot{\psi}cos\theta\ sin\phi\\ -\dot{\theta}sin\phi + \dot{\psi}cos\theta\ cos\phi\end{bmatrix} \quad (5)$$

The velocity of the mass center of any point on a body when mapped from the inertial frame to the body-fixed frame is given by **Equation (6)**,

$$\begin{bmatrix}V_x\\ V_y\\ V_z\end{bmatrix} = \begin{bmatrix}e\dot{\theta}\sin(\phi+\beta) - e\dot{\psi}\cos(\phi+\beta) + \dot{v}\sin\psi\, cos\theta - \dot{w}sin\theta\\ \dot{v}(sin\theta\ sin\phi\ sin\psi + cos\phi\ cos\psi) + \dot{w}cos\theta\ sin\phi + (\dot{\psi}sin\theta - \dot{\phi})esin\beta\\ \dot{v}(cos\phi\ sin\theta\ \sin\psi - sin\phi\ cos\psi) + \dot{w}cos\phi\ cos\theta + (-\dot{\psi}sin\theta + \dot{\phi})ecos\beta\end{bmatrix} \quad (6)$$

4.1.3. Kinematic constraints

Since the angular displacements ψ and θ are considered very small, ψ and θ can be expressed as shown in **Equation (7)** and **Equation (8)**:

$$\theta = -\frac{\partial w}{\partial x} \quad (7)$$

$$\psi = \frac{\partial v}{\partial x} \quad (8)$$

4.2. Energy expression

4.2.1. Shaft

As the shaft considered in this study is considered to be flexible, it will be characterized using the Kinetic energy as well as Potential energy.

The Kinetic energy of this shaft is given by (as shown in **Equation (9)**),

$$T = \frac{1}{2}\rho A\int_0^L V^2 dx + \frac{1}{2}I_{PS}\int_0^L {\omega_x}^2\, dx + \frac{1}{2}I_{DS}\int_0^L {\omega_y}^2 + {\omega_z}^2\, dx \quad (9)$$

This expression for Kinetic energy (as shown in **Equation (9)**) can be further simplified by substituting the expressions from **Equation (5)** as well as **Equation (6)**.

$$
\begin{aligned}
T = {} & \frac{1}{2}\rho A \int_0^L \dot{v}^2\, dx + \frac{1}{2}\rho A \int_0^L \dot{w}^2\, dx + \frac{1}{2}\rho A \int_0^L {e_s}^2\, \dot{\phi}^2 dx \\
& + \frac{1}{2}\rho A \int_0^L {e_s}^2\, \dot{\theta}^2 \sin^2(\phi + \beta_s)\, dx \\
& + \frac{1}{2}\rho A \int_0^L {e_s}^2\, \dot{\psi}^2 \left[\cos^2\theta \cos^2(\phi + \beta_s) + \sin^2\theta\right] dx \\
& + \frac{1}{2}\rho A \int_0^L e_s \dot{v}\, \dot{\phi}[-2\cos\psi \sin(\phi + \beta_s) \\
& + 2\sin\psi \sin\theta \cos(\phi + \beta_s)] dx \\
& + \frac{1}{2}\rho A \int_0^L e_s\, \dot{v}\dot{\theta}[2\sin\psi \cos\theta \sin(\phi + \beta_s)] dx \\
& + \frac{1}{2}\rho A \int_0^L e_s \dot{v}\, \dot{\psi}[-2\sin\psi \cos(\phi + \beta_s) \\
& + 2\cos\psi \sin\theta \sin(\phi + \beta_s)] dx \\
& + \frac{1}{2}\rho A \int_0^L e_s\, \dot{w}\dot{\phi}[2\cos\theta \cos(\phi + \beta_s)] dx \\
& + \frac{1}{2}\rho A \int_0^L e_s\, \dot{w}\dot{\theta}[-2\sin\theta \sin(\phi + \beta_s)] dx \\
& + \frac{1}{2}\rho A \int_0^L {e_s}^2\, \dot{\theta}\dot{\psi}[-2\cos\theta \cos(\phi + \beta_s) \sin(\phi + \beta_s)] dx \\
& + \frac{1}{2}\rho A \int_0^L {e_s}^2\, \dot{\psi}\dot{\phi}[-2\sin\theta] dx \\
& + \frac{1}{2} I_{PS} \int_0^L [\dot{\phi}^2 - 2\dot{\psi}\dot{\phi}\sin\theta + \dot{\psi}^2 \sin^2\theta]\, dx \\
& + \frac{1}{2} I_{DS} \int_0^L [\dot{\theta}^2 + \dot{\psi}^2 \cos^2\theta]\, dx
\end{aligned}
\qquad (10)
$$

Similarly, the potential energy of the shaft is given by (as shown in **Equation (11)**),

$$
V = \frac{EI}{2} \int_0^L \left[\left(\frac{\partial^2 v}{\partial x^2} \right)^2 + \left(\frac{\partial^2 w}{\partial x^2} \right)^2 \right] dx + \frac{GJ}{2} \int_0^L \left(\frac{\partial \phi}{\partial x} \right)^2 dx \qquad (11)
$$

4.2.2. Disc

Since both discs are assumed to be rigid it will be characterized by Kinetic energy only.

The kinetic energy of the first disc [Unbalanced disc] is given by (as shown in **Equation (12)**),

$$
\begin{aligned}
T = \frac{1}{2}M_{D1}\int_0^L \dot{v}^2\,[\cos^2\theta\cos^2\psi + \sin^2\theta]\delta\left(x-\frac{L}{3}\right)dx \\
+\frac{1}{2}M_{D1}\int_0^L 2e_D\dot{v}\,\dot{\phi}[-\cos\psi\sin(\phi+\beta_D) \\
+\sin\psi\sin\theta\cos(\phi+\beta_D)]\delta\left(x-\frac{L}{3}\right)dx \\
+\frac{1}{2}M_{D1}\int_0^L 2e_D\dot{v}\,\dot{\psi}[\sin\theta\cos\psi\sin(\phi+\beta_D) \\
-\sin^2\theta\sin\psi\cos(\phi+\beta_D)]\delta\left(x-\frac{L}{3}\right)dx \\
+\frac{1}{2}M_{D1}\int_0^L 2\dot{v}\,\dot{w}\sin\theta\cos\theta\sin\psi\,\delta\left(x-\frac{L}{3}\right)dx \\
+\frac{1}{2}M_{D1}\int_0^L {e_D}^2\,\dot{\phi}^2\delta\left(x-\frac{L}{3}\right)dx \\
+\frac{1}{2}M_{D1}\int_0^L 2{e_D}^2\,\dot{\phi}\dot{\psi}\sin\theta\,\delta\left(x-\frac{L}{3}\right)dx \\
+\frac{1}{2}M_{D1}\int_0^L 2e_D\dot{\phi}\,\dot{w}\cos\theta\cos(\phi+\beta_D)\,\delta\left(x-\frac{L}{3}\right)dx \\
+\frac{1}{2}M_{D1}\int_0^L {e_D}^2\,\dot{\psi}^2\sin^2\theta\,\delta\left(x-\frac{L}{3}\right)dx \\
+\frac{1}{2}M_{D1}\int_0^L -2e_D\dot{\psi}\,\dot{w}\sin\theta\cos\theta\cos(\phi+\beta_D)\,\delta\left(x-\frac{L}{3}\right)dx \\
+\frac{1}{2}M_{D1}\int_0^L \dot{w}^2\cos^2\theta\delta\left(x-\frac{L}{3}\right)dx \\
+\frac{1}{2}I_{PD1}\int_0^L [\dot{\phi}^2 - 2\dot{\psi}\dot{\phi}\sin\theta + \dot{\psi}^2\sin^2\theta]\,\delta\left(x-\frac{L}{3}\right)dx \\
+\frac{1}{2}I_{DD1}\int_0^L [\dot{\theta}^2 + \dot{\psi}^2\cos^2\theta]\delta\left(x-\frac{L}{3}\right)dx
\end{aligned}
\tag{12}
$$

Similarly, the kinetic energy of the second disc [Balanced disc] is given by (as shown in **Equation (13)**),

$$
\begin{aligned}
T = \frac{1}{2}M_{D2}\int_0^L \dot{v}^2\,[\cos^2\theta\cos^2\psi + \sin^2\theta]\delta(x-L)dx \\
+\frac{1}{2}M_{D2}\int_0^L 2\dot{v}\,\dot{w}\sin\theta\cos\theta\sin\psi\,\delta(x-L)\,dx \\
+\frac{1}{2}M_{D2}\int_0^L \dot{w}^2\cos^2\theta\delta(x-L)\,dx \\
+\frac{1}{2}I_{PD2}\int_0^L [\dot{\phi}^2 - 2\dot{\psi}\dot{\phi}\sin\theta + \dot{\psi}^2\sin^2\theta]\,\delta(x-L)dx \\
+\frac{1}{2}I_{DD2}\int_0^L [\dot{\theta}^2 + \dot{\psi}^2\cos^2\theta]\delta(x-L)\,dx
\end{aligned}
\tag{13}
$$

4.2.3. Non-conservatives

The non-conservatives in the shaft due to torque, due to eccentricity, and due to eccentricity in the discs are given by (as shown in **Equation (14)**, **Equation (15),** and **Equation (16)**)

$$W_{nc} = \int_0^L T(\phi - \psi sin\theta)\delta\left(x - \frac{L}{3}\right)dx \tag{14}$$

$$W_{nc} = \int_0^L F_{Shaft,y} v dx + \int_0^L F_{Shaft,z} w dx \tag{15}$$

$$W_{nc} = \int_0^L F_{Disc,y} v\delta\left(x - \frac{L}{3}\right)dx + \int_0^L F_{Disc,z} w\delta\left(x - \frac{L}{3}\right)dx \tag{16}$$

4.2.4. Lagrangian

From Kinetic energy as well as Potential Energy of Shaft along with Kinetic energy of discs, the Lagrangian is given by (as shown in **Equation (17)**),

$$L = \sum T - \sum V \tag{17}$$

The Lagrangian comprises a total of **31 Terms from Kinetic energy** and **2 Terms from Potential Energy**.

4.3. Extended Hamilton's principle

Using the Extended Hamilton's principle, the equations of motion can be obtained. The applied Extended Hamilton's principle for individual terms from energy expressions and non-conservatives is as shown below,

4.3.1. Extended Hamilton's principle for kinetic energy

First Term:

$$\int_{t_1}^{t_2} \delta\left(\int_0^L \frac{1}{2}\rho A\, \dot{v}^2 dx\right)dt = \int_{t_1}^{t_2}\int_0^L \frac{1}{2}\rho A\, \delta(\dot{v}^2)dxdt = \int_0^L \int_{t_1}^{t_2} \rho A\, \dot{v}\delta(\dot{v})dtdx$$

$$= \rho A \int_0^L \left(\dot{v}\delta v\Big|_{t_1}^{t_2} - \int_{t_1}^{t_2} \ddot{v}\, \delta v dt\right)dx = -\rho A \int_0^L \int_{t_1}^{t_2} \ddot{v}\delta v dx dt = \int_0^L \int_{t_1}^{t_2} -m\ddot{v}\delta v dx dt$$

Second Term:

$$\int_{t_1}^{t_2} \delta \left(\int_0^L \frac{1}{2} \rho A \, \dot{w}^2 dx \right) dt = \int_{t_1}^{t_2} \int_0^L \frac{1}{2} \rho A \, \delta(\dot{w}^2) dx dt = \int_0^L \int_{t_1}^{t_2} \rho A \, \dot{w} \delta(\dot{w}) dt dx$$

$$= \rho A \int_0^L \left(\dot{w} \delta w \Big|_{t_1}^{t_2} - \int_{t_1}^{t_2} \ddot{w} \, \delta w dt \right) dx = -\rho A \int_0^L \int_{t_1}^{t_2} \ddot{w} \delta w dx dt = \int_0^L \int_{t_1}^{t_2} -m \ddot{w} \delta w dx dt$$

Third Term:

$$\int_{t_1}^{t_2} \delta \left(\int_0^L \frac{1}{2} \rho A {e_s}^2 \, \dot{\phi}^2 dx \right) dt = \int_{t_1}^{t_2} \int_0^L \frac{1}{2} \rho A {e_s}^2 \, \delta(\dot{\phi}^2) dx dt = \int_0^L \int_{t_1}^{t_2} \rho A \, {e_s}^2 \, \dot{\phi} \delta(\dot{\phi}) dt dx$$

$$= \rho A {e_s}^2 \int_0^L \left(\dot{\phi} \delta \phi \Big|_{t_1}^{t_2} - \int_{t_1}^{t_2} \ddot{\phi} \, \delta \phi dt \right) dx$$

$$= -\rho A {e_s}^2 \int_0^L \int_{t_1}^{t_2} \ddot{\phi} \delta \phi dx dt = \int_0^L \int_{t_1}^{t_2} -m {e_s}^2 \ddot{\phi} \delta \phi dx dt$$

Fourth Term:

$$\int_{t_1}^{t_2} \delta \left(\frac{1}{2} \rho A \int_0^L {e_s}^2 \, \dot{\theta}^2 \sin^2(\phi + \beta_s) \, dx \right) dt = \boxed{\text{Higher Order Term}}$$

Fifth Term:

$$\int_{t_1}^{t_2} \delta \left(\frac{1}{2} \rho A \int_0^L {e_s}^2 \, \dot{\psi}^2 \left[\cos^2\theta \cos^2(\phi + \beta_s) + \sin^2\theta \right] dx \right) dt = \boxed{\text{Higher Order Term}}$$

Sixth Term:

$$\int_{t_1}^{t_2} \delta \left(\frac{1}{2} \rho A \int_0^L e_s \dot{v} \, \dot{\phi} [-2 \cos\psi \sin(\phi + \beta_s) + 2 \sin\psi \sin\theta \cos(\phi + \beta_s)] dx \right) dt$$

$$= \int_{t_1}^{t_2} \delta \left(\frac{1}{2} \rho A \int_0^L e_s \dot{v} \, \dot{\phi} [-2 \cos\psi \sin(\phi + \beta_s)] dx \right) dt$$

$$+ \boxed{\text{Higher Order Term}}$$

$$= \int_0^L \delta \left(\int_{t_1}^{t_2} -\rho A \, e_s \dot{v} \dot{\phi} \sin(\phi + \beta_s) \right) dt$$

$$= -\rho A e_s \sin(\phi + \beta_s) \int_0^L \int_{t_1}^{t_2} \left(\dot{v} \delta \dot{\phi} + \dot{\phi} \delta \dot{v} \right) dt dx$$

$$= -me_s \sin(\phi + \beta_s) \int_0^L \left(\dot{v}\delta\phi \Big|_{t_1}^{t_2} - \int_{t_1}^{t_2} \ddot{v}\, \delta\phi dt \right) dx$$

$$- me_s \sin(\phi + \beta_s) \int_0^L \left(\dot{\phi}\delta v \Big|_{t_1}^{t_2} - \int_{t_1}^{t_2} \ddot{\phi}\, \delta v dt \right) dx$$

$$= \int_0^L \int_{t_1}^{t_2} me_s \ddot{v} \sin(\phi + \beta_s)\, \delta\phi dx dt + \int_0^L \int_{t_1}^{t_2} \frac{\partial}{\partial t}\left(me_s \dot{\phi} \sin(\phi + \beta_s)\right) \delta v dx dt$$

Seventh Term:

$$\int_{t_1}^{t_2} \delta \left(\frac{1}{2}\rho A \int_0^L e_s\, \dot{v}\dot{\theta}[2 \sin\psi \cos\theta \sin(\phi + \beta_s)] dx \right) dt = \boxed{\text{Higher Order Term}}$$

Eighth Term:

$$\int_{t_1}^{t_2} \delta \left(\frac{1}{2}\rho A \int_0^L e_s \dot{v}\, \dot{\psi}[-2 \sin\psi \cos(\phi + \beta_s) + 2 \cos\psi \sin\theta \sin(\phi + \beta_s)] dx \right) dt$$

$$= \boxed{\text{Higher Order Term}}$$

Ninth Term:

$$\int_{t_1}^{t_2} \delta \left(\frac{1}{2}\rho A \int_0^L e_s\, \dot{w}\dot{\phi}[2 \cos\theta \cos(\phi + \beta_s)] dx \right) dt = \int_0^L \delta \left(\int_{t_1}^{t_2} \rho A\, e_s \dot{w}\dot{\phi} \cos(\phi + \beta_s) \right) dt$$

$$= \rho A e_s \cos(\phi + \beta_s) \int_0^L \int_{t_1}^{t_2} \left(\dot{w}\delta\dot{\phi} + \dot{\phi}\delta\dot{w} \right) dt dx$$

$$= me_s \cos(\phi + \beta_s) \int_0^L \left(\dot{w}\delta\phi \Big|_{t_1}^{t_2} - \int_{t_1}^{t_2} \ddot{w}\, \delta\phi dt \right) dx$$

$$+ me_s \cos(\phi + \beta_s) \int_0^L \left(\dot{\phi}\delta w \Big|_{t_1}^{t_2} - \int_{t_1}^{t_2} \ddot{\phi}\, \delta w dt \right) dx$$

$$= -\int_0^L \int_{t_1}^{t_2} me_s \ddot{w} \cos(\phi + \beta_s)\, \delta\phi dx dt - \int_0^L \int_{t_1}^{t_2} \frac{\partial}{\partial t}\left(me_s \dot{\phi} \cos(\phi + \beta_s)\right) \delta w dx dt$$

Tenth Term:

$$\int_{t_1}^{t_2} \delta \left(\frac{1}{2}\rho A \int_0^L e_s\, \dot{w}\dot{\theta}[-2 \sin\theta \sin(\phi + \beta_s)] dx \right) dt = \boxed{\text{Higher Order Term}}$$

Eleventh Term:

$$\int_{t_1}^{t_2} \delta \left(\frac{1}{2}\rho A \int_0^L {e_s}^2\, \dot{\theta}\dot{\psi}[-2 \cos\theta \cos(\phi + \beta_s) \sin(\phi + \beta_s)] dx \right) dt = \boxed{\text{Higher Order Term}}$$

Twelfth Term:

$$\int_{t_1}^{t_2} \delta \left(\frac{1}{2} \rho A \int_0^L {e_s}^2 \, \dot{\psi} \dot{\phi} [-2 \sin\theta] dx \right) dt = \boxed{\text{Higher Order Term}}$$

Thirteenth Term:

$$\int_{t_1}^{t_2} \delta \left(\frac{1}{2} I_{PS} \int_0^L \left[\dot{\phi}^2 - 2\dot{\psi}\dot{\phi} \sin\theta + \dot{\psi}^2 \sin^2\theta \right] dx \right) dt$$

$$= \int_{t_1}^{t_2} \delta \left(\frac{1}{2} I_{PS} \int_0^L \left[\dot{\phi}^2 - 2\dot{\psi}\dot{\phi} \sin\theta \right] dx \right) dt + \boxed{\text{Higher Order Term}}$$

$$= \int_{t_1}^{t_2} \delta \left(\frac{1}{2} I_{PS} \int_0^L \left[\dot{\phi}^2 - 2\dot{\psi}\dot{\phi}\dot{\theta} \right] dx \right) dt$$

$$= -\int_0^L \int_{t_1}^{t_2} I_{PS} \ddot{\phi} \delta\phi \, dx dt + \int_0^L \int_{t_1}^{t_2} I_{PS} \delta(\dot{\phi} \dot{v}' w') dx dt$$

$$= -\int_0^L \int_{t_1}^{t_2} I_{PS} \ddot{\phi} \delta\phi \, dx dt + \int_0^L \int_{t_1}^{t_2} I_{PS} \dot{v}' w' \delta\dot{\phi} \, dx dt + \int_0^L \int_{t_1}^{t_2} I_{PS} \dot{\phi} w' \delta\dot{v}' dx dt$$
$$+ \int_0^L \int_{t_1}^{t_2} I_{PS} \dot{\phi} \dot{v}' \delta w' dx dt$$

$$= -\int_0^L \int_{t_1}^{t_2} I_{PS} \ddot{\phi} \delta\phi \, dx dt + I_{PS} \int_0^L \left(w' \dot{v}' \delta\phi \Big|_{t_1}^{t_2} - \int_{t_1}^{t_2} \frac{\partial}{\partial t} (w' \dot{v}') \, \delta\phi dt \right) dx$$
$$+ I_{PS} \int_{t_1}^{t_2} \left(\dot{\phi} \dot{v}' \delta w \Big|_0^L - \int_0^L \left(\dot{\phi} \dot{v}' \right)' \delta w dt \right) dx$$
$$+ I_{PS} \int_{t_1}^{t_2} \left(\dot{\phi} w' \delta\dot{v} \Big|_0^L - \int_0^L \frac{\partial}{\partial x} \left(\dot{\phi} w' \right) \delta\dot{v} dt \right) dx$$

$$= -\int_0^L \int_{t_1}^{t_2} I_{PS} \ddot{\phi} \delta\phi \, dx dt - I_{PS} \int_0^L \left(\int_{t_1}^{t_2} \frac{\partial}{\partial t} (w' \dot{v}') \, \delta\phi dt \right) dx$$
$$- I_{PS} \int_{t_1}^{t_2} \left(\int_0^L \left(\dot{\phi} \dot{v}' \right)' \delta w dt \right) dx - I_{PS} \int_{t_1}^{t_2} \left(\int_0^L \frac{\partial}{\partial x} \left(\dot{\phi} w' \right) \delta\dot{v} dt \right) dx$$
$$+ \boxed{\text{Boundary Conditions}}$$

$$= -\int_0^L \int_{t_1}^{t_2} I_{PS}\ddot{\phi}\delta\phi dx dt - I_{PS}\int_0^L \left(\int_{t_1}^{t_2} \frac{\partial}{\partial t}(w'\dot{v}')\,\delta\phi dt\right) dx$$

$$- I_{PS}\int_{t_1}^{t_2}\left(\int_0^L (\dot{\phi}\dot{v}')'\,\delta w dt\right) dx$$

$$- I_{PS}\int_0^L \left(\frac{\partial}{\partial x}(\dot{\phi}w')\delta v\,\Big|_{t_1}^{t_2} - \int_{t_1}^{t_2}\frac{\partial}{\partial t}\frac{\partial}{\partial x}(\dot{\phi}w')\,\delta v dt\right) dx$$

$$+ \boxed{\text{Boundary Conditions}}$$

$$= -\int_0^L \int_{t_1}^{t_2} I_{PS}\ddot{\phi}\delta\phi dx dt - I_{PS}\int_0^L \left(\int_{t_1}^{t_2} \frac{\partial}{\partial t}(w'\dot{v}')\,\delta\phi dt\right) dx$$

$$- I_{PS}\int_{t_1}^{t_2}\left(\int_0^L (\dot{\phi}\dot{v}')'\,\delta w dt\right) dx + I_{PS}\int_0^L \left(\int_{t_1}^{t_2}\frac{\partial}{\partial t}\frac{\partial}{\partial x}(\dot{\phi}w')\,\delta v dt\right) dx$$

$$+ \boxed{\text{Boundary Conditions}}$$

$$-\int_0^L \int_{t_1}^{t_2} I_{PS}\ddot{\phi}\delta\phi dx dt - I_{PS}\int_0^L \left(\int_{t_1}^{t_2} \frac{\partial}{\partial t}(w'\dot{v}')\,\delta\phi dt\right) dx - I_{PS}\int_{t_1}^{t_2}\left(\int_0^L (\dot{\phi}\dot{v}')'\,\delta w dt\right) dx$$

$$+ I_{PS}\int_0^L \left(\int_{t_1}^{t_2} (\ddot{\phi}w' + \dot{\phi}\dot{w}')'\,\delta v dt\right) dx + \boxed{\text{Boundary Conditions}}$$

Fourteenth Term:

$$\int_{t_1}^{t_2}\delta\left(\frac{1}{2}I_{DS}\int_0^L [\dot{\theta}^2 + \dot{\psi}^2\cos^2\theta]\,dx\right) dt = \int_{t_1}^{t_2}\delta\left(\frac{1}{2}I_{DS}\int_0^L [\dot{\theta}^2 + \dot{\psi}^2]\,dx\right) dt$$

$$= \int_{t_1}^{t_2}\delta\left(\frac{1}{2}I_{DS}\int_0^L [(\dot{w})'^2 + (\dot{v})'^2]\,dx\right) dt = \int_0^L\int_{t_1}^{t_2} I_{DS}\delta(\dot{w})'^2 dx dt + \int_0^L\int_{t_1}^{t_2} I_{DS}\delta(\dot{v})'^2 dx dt$$

$$= I_{DS}\int_{t_1}^{t_2}\left(\dot{w}'\delta\dot{w}\,\Big|_0^L - \int_0^L \dot{w}''\,\delta\dot{w}dt\right) dx + I_{DS}\int_{t_1}^{t_2}\left(\dot{v}'\delta\dot{v}\,\Big|_0^L - \int_0^L \dot{v}''\,\delta\dot{v}dt\right) dx$$

$$= I_{DS}\int_{t_1}^{t_2}\left(-\int_0^L \dot{w}''\,\delta\dot{w}dt\right) dx + I_{DS}\int_{t_1}^{t_2}\left(-\int_0^L \dot{v}''\,\delta\dot{v}dt\right) dx + \boxed{\text{Boundary Conditions}}$$

$$= -I_{DS}\int_{t_1}^{t_2}\left(\dot{w}''\delta w\,\Big|_0^L - \int_0^L \ddot{w}''\,\delta w dt\right) dx - I_{DS}\int_{t_1}^{t_2}\left(\dot{v}''\delta v\,\Big|_0^L - \int_0^L \ddot{v}''\,\delta v dt\right) dx$$

$$+ \boxed{\text{Boundary Conditions}}$$

$$= I_{DS}\int_{t_1}^{t_2}\left(\int_0^L \ddot{w}''\,\delta w dt\right) dx + I_{DS}\int_{t_1}^{t_2}\left(\int_0^L \ddot{v}''\,\delta v dt\right) dx + \boxed{\text{Boundary Conditions}}$$

Fifteenth Term:

$$\int_{t_1}^{t_2}\delta\left(\frac{1}{2}M_{D1}\int_0^L \dot{v}^2\left[\cos^2\theta\cos^2\psi+\sin^2\theta\right]\delta\left(x-\frac{L}{3}\right)dx\right)dt$$

$$=\int_{t_1}^{t_2}\delta\left(\frac{1}{2}M_{D1}\int_0^L\left[\dot{v}^2+\dot{v}^2\theta^2\right]\delta\left(x-\frac{L}{3}\right)dx\right)dt$$

$$=\int_0^L\int_{t_1}^{t_2}-M_{D1}\ddot{v}\left(x-\frac{L}{3}\right)\delta v dx dt+\int_{t_1}^{t_2}\delta\left(\frac{1}{2}M_{D1}\int_0^L\left[\dot{v}^2w'^2\right]\delta\left(x-\frac{L}{3}\right)dx\right)dt$$

$$=\int_0^L\int_{t_1}^{t_2}-M_{D1}\ddot{v}\delta\left(x-\frac{L}{3}\right)\delta v dx dt+\frac{1}{2}M_{D1}\int_0^L\int_{t_1}^{t_2}2\left(\dot{v}^2w'\delta w'+w'^2\dot{v}\delta\dot{v}\right)\delta\left(x-\frac{L}{3}\right)dx dt$$

$$=\int_0^L\int_{t_1}^{t_2}-M_{D1}\ddot{v}\delta\left(x-\frac{L}{3}\right)\delta v dx dt+M_{D1}\delta\left(x-\frac{L}{3}\right)\int_{t_1}^{t_2}\left(\dot{v}^2w'\delta w\Big|_0^L-\int_0^L\dot{v}^2w''\,\delta w dt\right)dx$$

$$+M_{D1}\delta\left(x-\frac{L}{3}\right)\int_0^L\left(w'^2\dot{v}\delta v\Big|_{t_1}^{t_2}-\int_{t_1}^{t_2}\left(w'^2\dot{v}\right)'\delta v dt\right)dx$$

$$=\int_0^L\int_{t_1}^{t_2}-M_{D1}\ddot{v}\delta\left(x-\frac{L}{3}\right)\delta v dx dt-M_{D1}\delta\left(x-\frac{L}{3}\right)\int_{t_1}^{t_2}\left(\int_0^L\left(\dot{v}^2w'\right)'\delta w dt\right)dx$$

$$-M_{D1}\delta\left(x-\frac{L}{3}\right)\int_0^L\left(\int_{t_1}^{t_2}\frac{\partial}{\partial t}\left(w'^2\dot{v}\right)\delta v dt\right)dx+\boxed{\text{Boundary Conditions}}$$

Sixteenth Term:

$$\int_{t_1}^{t_2}\delta\left(\frac{1}{2}M_{D1}\int_0^L 2e_D\dot{v}\,\dot{\phi}[-\cos\psi\sin(\phi+\beta_D)+\sin\psi\sin\theta\cos(\phi+\beta_D)]\delta\left(x-\frac{L}{3}\right)dx\right)dt$$

$$=\int_{t_1}^{t_2}\delta\left(\frac{1}{2}M_{D1}\int_0^L 2e_D\dot{v}\,\dot{\phi}[-\cos\psi\sin(\phi+\beta_D)]\delta\left(x-\frac{L}{3}\right)dx\right)dt$$

$$=\int_0^L\int_{t_1}^{t_2}M_{D1}e_D\ddot{v}\sin(\phi+\beta_D)\delta\left(x-\frac{L}{3}\right)\delta\phi dx dt$$

$$+\int_0^L\int_{t_1}^{t_2}\frac{\partial}{\partial t}\left(M_{D1}e_D\dot{\phi}\sin(\phi+\beta_D)\right)\delta\left(x-\frac{L}{3}\right)\delta v dx dt$$

Seventeenth Term:

$$\int_{t_1}^{t_2}\delta\left(\frac{1}{2}M_{D1}\int_0^L 2e_D\dot{v}\,\dot{\psi}[\sin\theta\cos\psi\sin(\phi+\beta_D)-\sin^2\theta\sin\psi\cos(\phi+\beta_D)]\delta\left(x-\frac{L}{3}\right)dx\right)dt=\boxed{\text{Higher Order Term}}$$

Eighteenth Term:

$$\int_{t_1}^{t_2} \delta \left(\frac{1}{2} M_{D1} \int_0^L 2\dot{v}\, \dot{w} \sin\theta \cos\theta \sin\psi\, \delta \left(x - \frac{L}{3} \right) dx \right) dt = \boxed{\text{Higher Order Term}}$$

Nineteenth Term:

$$\int_{t_1}^{t_2} \delta \left(\frac{1}{2} M_{D1} \int_0^L {e_D}^2\, \dot{\phi}^2 \delta \left(x - \frac{L}{3} \right) dx \right) dt = \int_0^L \int_{t_1}^{t_2} -M_{D1} {e_D}^2 \delta \left(x - \frac{L}{3} \right) \ddot{\phi} \delta\phi\, dx dt$$

Twentieth Term:

$$\int_{t_1}^{t_2} \delta \left(\frac{1}{2} M_{D1} \int_0^L 2{e_D}^2\, \dot{\phi}\dot{\psi} \sin\theta\, \delta \left(x - \frac{L}{3} \right) dx \right) dt = \boxed{\text{Higher Order Term}}$$

Twenty-first Term:

$$\int_{t_1}^{t_2} \delta \left(\frac{1}{2} M_{D1} \int_0^L 2 e_D \dot{\phi}\, \dot{w} \cos\theta \cos(\phi + \beta_D)\, \delta \left(x - \frac{L}{3} \right) dx \right) dt$$

$$= -\int_0^L \int_{t_1}^{t_2} M_{D1} e_D \ddot{w} \cos(\phi + \beta_D) \delta \left(x - \frac{L}{3} \right) \delta\phi\, dx dt$$

$$- \int_0^L \int_{t_1}^{t_2} \frac{\partial}{\partial t} \left(M_{D1} e_D \dot{\phi} \cos(\phi + \beta_D) \right) \delta \left(x - \frac{L}{3} \right) \delta w\, dx dt$$

Twenty-second Term:

$$\int_{t_1}^{t_2} \delta \left(\frac{1}{2} M_{D1} \int_0^L {e_D}^2\, \dot{\psi}^2 \sin^2\theta\, \delta \left(x - \frac{L}{3} \right) dx \right) dt = \boxed{\text{Higher Order Term}}$$

Twenty-third Term:

$$\int_{t_1}^{t_2} \delta \left(\frac{1}{2} M_{D1} \int_0^L -2 e_D \dot{\psi}\, \dot{w} \sin\theta \cos\theta \cos(\phi + \beta_D)\, \delta \left(x - \frac{L}{3} \right) dx \right) dt$$

$$= \boxed{\text{Higher Order Term}}$$

Twenty-fourth Term:

$$\int_{t_1}^{t_2} \delta \left(\frac{1}{2} M_{D1} \int_0^L \dot{w}^2 \cos^2\theta \delta \left(x - \frac{L}{3} \right) dx \right) dt = \int_0^L \int_{t_1}^{t_2} -M_{D1} \ddot{w} \delta \left(x - \frac{L}{3} \right) \delta w\, dx dt$$

Twenty-fifth Term:

$$\int_{t_1}^{t_2} \delta \left(\frac{1}{2} I_{PD1} \int_0^L [\dot{\phi}^2 - 2\dot{\psi}\dot{\phi} \sin\theta + \dot{\psi}^2 \sin^2\theta]\, \delta \left(x - \frac{L}{3} \right) dx \right) dt$$

$$= \int_0^L \int_{t_1}^{t_2} -I_{PD1}\ddot{\phi}\delta\left(x-\frac{L}{3}\right)\delta\phi dxdt - \int_0^L \int_{t_1}^{t_2} I_{PD1}\frac{\partial}{\partial t}(w'\dot{v}')\delta\left(x-\frac{L}{3}\right)\delta\phi dxdt$$
$$- \int_0^L \int_{t_1}^{t_2} I_{PD1}(\dot{\phi}\dot{v}')'\delta\left(x-\frac{L}{3}\right)\delta w dxdt$$
$$+ \int_0^L \int_{t_1}^{t_2} I_{PD1}(w'\ddot{\phi})'\delta\left(x-\frac{L}{3}\right)\delta v dxdt$$
$$+ \int_0^L \int_{t_1}^{t_2} I_{PD1}(\dot{\phi}\dot{w}')'\delta\left(x-\frac{L}{3}\right)\delta v dxdt + \boxed{\text{Boundary Conditions}}$$

Twenty-sixth Term:

$$\int_{t_1}^{t_2} \delta\left(\frac{1}{2}I_{DD1}\int_0^L [\dot{\theta}^2 + \dot{\psi}^2\cos^2\theta]\delta\left(x-\frac{L}{3}\right)dx\right)dt$$

$$= I_{DD1}\delta\left(x-\frac{L}{3}\right)\int_{t_1}^{t_2}\left(\int_0^L \ddot{w}''\,\delta w dt\right)dx + I_{DD1}\delta\left(x-\frac{L}{3}\right)\int_{t_1}^{t_2}\left(\int_0^L \ddot{v}''\,\delta v dt\right)dx$$
$$+ \boxed{\text{Boundary Conditions}}$$

Twenty-seventh Term:

$$\int_{t_1}^{t_2} \delta\left(\frac{1}{2}M_{D2}\int_0^L \dot{v}^2\,[\cos^2\theta\cos^2\psi + \sin^2\theta]\delta(x-L)dx\right)dt$$

$$= \int_0^L \int_{t_1}^{t_2} -M_{D2}\ddot{v}\delta(x-L)\delta v dxdt - M_{D2}\delta(x-L)\int_{t_1}^{t_2}\left(\int_0^L (\dot{v}^2 w')'\,\delta w dt\right)dx$$
$$- M_{D2}\delta(x-L)\int_0^L\left(\int_{t_1}^{t_2}\frac{\partial}{\partial t}(w'^2\dot{v})\,\delta v dt\right)dx + \boxed{\text{Boundary Conditions}}$$

Twenty-eighth Term:

$$\int_{t_1}^{t_2} \delta\left(\frac{1}{2}M_{D2}\int_0^L 2\dot{v}\,\dot{w}\sin\theta\cos\theta\sin\psi\,\delta(x-L)\,dx\right)dt = \boxed{\text{Higher Order Term}}$$

Twenty-ninth Term:

$$\int_{t_1}^{t_2} \delta\left(\frac{1}{2}M_{D2}\int_0^L \dot{w}^2\cos^2\theta\delta(x-L)\,dx\right)dt = \int_0^L \int_{t_1}^{t_2} -M_{D2}\ddot{w}\delta(x-L)\delta w dxdt$$

Thirtieth Term:

$$\int_{t_1}^{t_2} \delta\left(\frac{1}{2}I_{PD2}\int_0^L [\dot{\phi}^2 - 2\dot{\psi}\dot{\phi}\sin\theta + \dot{\psi}^2\sin^2\theta]\,\delta(x-L)dx\right)dt$$

$$= \int_0^L \int_{t_1}^{t_2} -I_{PD2}\ddot{\phi}\delta(x-L)\delta\phi dxdt - \int_0^L \int_{t_1}^{t_2} I_{PD2}\frac{\partial}{\partial t}(w'\dot{v}')\delta(x-L)\delta\phi dxdt$$

$$- \int_0^L \int_{t_1}^{t_2} I_{PD2}\left(\dot{\phi}\dot{v}'\right)'\delta(x-L)\delta w dxdt$$

$$+ \int_0^L \int_{t_1}^{t_2} I_{PD2}\left(w'\ddot{\phi}\right)'\delta(x-L)\delta v dxdt$$

$$+ \int_0^L \int_{t_1}^{t_2} I_{PD2}\left(\dot{\phi}\dot{w}'\right)'\delta(x-L)\delta v dxdt + \boxed{\text{Boundary Conditions}}$$

Thirty-first Term:

$$\int_{t_1}^{t_2} \delta\left(\frac{1}{2}I_{DD2}\int_0^L [\dot{\theta}^2 + \dot{\psi}^2\cos^2\theta]\delta(x-L)\,dx\right)dt$$

$$= I_{DD2}\delta(x-L)\int_{t_1}^{t_2}\left(\int_0^L \ddot{w}''\,\delta w dt\right)dx + I_{DD2}\delta(x-L)\int_{t_1}^{t_2}\left(\int_0^L \ddot{v}''\,\delta v dt\right)dx$$

$$+ \boxed{\text{Boundary Conditions}}$$

4.3.2. Extended Hamilton's principle for potential energy

Thirty-second Term:

$$\int_{t_1}^{t_2} \delta\left(\frac{EI}{2}\int_0^L \left[\left(\frac{\partial^2 v}{\partial x^2}\right)^2 + \left(\frac{\partial^2 w}{\partial x^2}\right)^2\right]dx\right)dt$$

$$= \int_0^L \int_{t_1}^{t_2} EI\left(\frac{\partial^2 v}{\partial x^2}\right)\delta\left(\frac{\partial^2 v}{\partial x^2}\right)dtdx + \int_0^L \int_{t_1}^{t_2} EI\left(\frac{\partial^2 w}{\partial x^2}\right)\delta\left(\frac{\partial^2 w}{\partial x^2}\right)dtdx$$

$$= EI\int_{t_1}^{t_2}\left(\left(\frac{\partial^2 v}{\partial x^2}\right)\delta\left(\frac{\partial v}{\partial x}\right)\Big|_0^L - \int_0^L \left(\frac{\partial^3 v}{\partial x^3}\right)\delta\left(\frac{\partial v}{\partial x}\right)dx\right)dt$$

$$+ EI\int_{t_1}^{t_2}\left(\left(\frac{\partial^2 w}{\partial x^2}\right)\delta\left(\frac{\partial w}{\partial x}\right)\Big|_0^L - \int_0^L \left(\frac{\partial^3 w}{\partial x^3}\right)\delta\left(\frac{\partial w}{\partial x}\right)dx\right)dt$$

$$= -EI\int_{t_1}^{t_2}\left(\int_0^L \left(\frac{\partial^3 v}{\partial x^3}\right)\delta\left(\frac{\partial v}{\partial x}\right)dx\right)dt - EI\int_{t_1}^{t_2}\left(\int_0^L \left(\frac{\partial^3 w}{\partial x^3}\right)\delta\left(\frac{\partial w}{\partial x}\right)dx\right)dt$$

$$+ \boxed{\text{Boundary Conditions}}$$

$$= -EI \int_{t_1}^{t_2} \left(\left(\frac{\partial^3 v}{\partial x^3} \right) \delta(v) \Big|_0^L + \int_0^L \left(\frac{\partial^4 v}{\partial x^4} \right) \delta(v)\, dx \right) dt$$

$$- EI \int_{t_1}^{t_2} \left(\left(\frac{\partial^3 w}{\partial x^3} \right) \delta(w) \Big|_0^L + \int_0^L \left(\frac{\partial^4 w}{\partial x^4} \right) \delta(w)\, dx \right) dt$$

$$= EI \int_{t_1}^{t_2} \left(\int_0^L \left(\frac{\partial^4 v}{\partial x^4} \right) \delta(v)\, dx \right) dt + EI \int_{t_1}^{t_2} \left(\int_0^L \left(\frac{\partial^4 w}{\partial x^4} \right) \delta(w)\, dx \right) dt$$

$$+ \boxed{\text{Boundary Conditions}}$$

Thirty-third Term:

$$\int_{t_1}^{t_2} \delta \left(\frac{GJ}{2} \int_0^L \left(\frac{\partial \phi}{\partial x} \right)^2 dx \right) dt = \int_0^L \int_{t_1}^{t_2} GJ \left(\frac{\partial \phi}{\partial x} \right) \delta \left(\frac{\partial \phi}{\partial x} \right) dt dx$$

$$= GJ \int_{t_1}^{t_2} \left(\left(\frac{\partial \phi}{\partial x} \right) \delta(\phi) \Big|_0^L - \int_0^L \left(\frac{\partial^2 \phi}{\partial x^2} \right) \delta(\phi)\, dx \right) dt$$

$$= -GJ \int_{t_1}^{t_2} \left(\int_0^L \left(\frac{\partial^2 \phi}{\partial x^2} \right) \delta(\phi)\, dx \right) dt + \boxed{\text{Boundary Conditions}}$$

4.3.3. Extended Hamilton's principle for non-conservatives

Thirty-fourth Term:

$$\int_{t_1}^{t_2} \delta \left(\int_0^L T(\phi - \psi sin\theta) dx \right) dt$$

$$= \int_0^L \int_{t_1}^{t_2} T\, \delta\phi dx dt + \int_0^L \int_{t_1}^{t_2} T\, w'\, \delta v' dx dt + \int_0^L \int_{t_1}^{t_2} T\, v'\, \delta w' dx dt$$

$$= \int_0^L \int_{t_1}^{t_2} T\, \delta\phi dx dt + T \int_{t_1}^{t_2} \left(w' \delta v \Big|_0^L - \int_0^L w''\, \delta v dt \right) dx$$

$$+ T \int_{t_1}^{t_2} \left(v' \delta w \Big|_0^L - \int_0^L v''\, \delta w dt \right) dx$$

$$= \int_0^L \int_{t_1}^{t_2} T\, \delta\phi dx dt - T \int_{t_1}^{t_2} \left(\int_0^L w''\, \delta v dt \right) dx - T \int_{t_1}^{t_2} \left(\int_0^L v''\, \delta w dt \right) dx$$

$$+ \boxed{\text{Boundary Conditions}}$$

Thirty-fifth Term:

$$\int_{t_1}^{t_2} \delta \left(\int_0^L F_{Shaft,y} v dx + \int_0^L F_{Shaft,z} w dx \right) dt$$
$$= \int_0^L \int_{t_1}^{t_2} F_{Shaft,y} \delta v dx dt + \int_0^L \int_{t_1}^{t_2} F_{Shaft,z} \delta w dx dt$$

Thirty-sixth Term:

$$\int_{t_1}^{t_2} \delta \left(\int_0^L F_{Disc,y} v \delta \left(x - \frac{L}{3} \right) dx + \int_0^L F_{Disc,z} w \delta \left(x - \frac{L}{3} \right) dx \right) dt$$
$$= \int_0^L \int_{t_1}^{t_2} F_{Disc,y} \delta \left(x - \frac{L}{3} \right) \delta v dx dt + \int_0^L \int_{t_1}^{t_2} F_{Disc,z} \delta \left(x - \frac{L}{3} \right) \delta w dx dt$$

4.4. Equation of motion

The equation of motion in three fundamental directions after application of the Extended Hamilton principle is given as shown in **Equation (18)**, **Equation (19)**, and **Equation (20)**.

$$\begin{aligned} EIv'''' + m\ddot{v} - I_{PS}\left(w'\ddot{\phi}\right)' - I_{PS}\left(\dot{\phi}\dot{w}'\right)' - I_{DS}(\ddot{v}')' \\ = \frac{\partial}{\partial t}\left(me_S\dot{\phi}\sin(\phi+\beta_S)\right) - M_{D1}\ddot{v}\delta\left(x-\frac{L}{3}\right) \\ - M_{D1}\frac{\partial}{\partial t}\left(w'^2\dot{v}\right)\delta\left(x-\frac{L}{3}\right) + \frac{\partial}{\partial t}\left(M_{D1}e_D\dot{\phi}\sin(\phi+\beta_D)\right) \\ + I_{PD1}\left(w'\ddot{\phi}\right)'\delta\left(x-\frac{L}{3}\right) + I_{PD1}\left(\dot{\phi}\dot{w}'\right)'\delta\left(x-\frac{L}{3}\right) \\ + I_{DD1}(\ddot{v}')'\delta\left(x-\frac{L}{3}\right) - M_{D2}\ddot{v}\delta(x-L) - M_{D2}\frac{\partial}{\partial t}\left(w'^2\dot{v}\right)\delta(x-L) \\ + I_{PD2}\left(w'\ddot{\phi}\right)'\delta\left(x-\frac{L}{3}\right) + I_{PD2}\left(\dot{\phi}\dot{w}'\right)'\delta\left(x-\frac{L}{3}\right) \\ + I_{DD2}(\ddot{v}')'\delta\left(x-\frac{L}{3}\right) - Tw''\delta\left(x-\frac{L}{3}\right) + F_{Shaft,y} \\ + F_{Disc,y}\delta\left(x-\frac{L}{3}\right) \end{aligned} \tag{18}$$

$$\begin{aligned} EIw'''' + m\ddot{w} + I_{PS}\left(\dot{\phi}\dot{v}'\right)' - I_{DS}(\ddot{w}')' \\ = -\frac{\partial}{\partial t}\left(me_S\dot{\phi}\cos(\phi+\beta_S)\right) - M_{D1}\ddot{w}\delta\left(x-\frac{L}{3}\right) \\ - M_{D1}(w'\dot{v}^2)'\delta\left(x-\frac{L}{3}\right) - \frac{\partial}{\partial t}\left(M_{D1}e_D\dot{\phi}\cos(\phi+\beta_D)\,\delta\left(x-\frac{L}{3}\right)\right) \\ - I_{PD1}\left(\dot{\phi}\dot{v}'\right)'\delta\left(x-\frac{L}{3}\right) + I_{DD1}(\ddot{w}')'\delta\left(x-\frac{L}{3}\right) - M_{D2}\ddot{w}\delta(x-L) \\ - M_{D2}(w'\dot{v}^2)'\delta(x-L) - I_{PD2}\left(\dot{\phi}\dot{v}'\right)'\delta(x-L) + I_{DD2}(\ddot{w}')'\delta(x-L) \\ - Tv''\delta\left(x-\frac{L}{3}\right) + F_{Shaft,z} + F_{Disc,z}\delta\left(x-\frac{L}{3}\right) \end{aligned} \tag{19}$$

$$
\begin{aligned}
GJ\phi'' - me_S{}^2\ddot{\phi} - I_{PS}\ddot{\phi} - I_{PS}\frac{\partial}{\partial t}(w'\dot{v}') \\
&= -me_S\ddot{v}\sin(\phi+\beta_S) + me_S\ddot{w}\cos(\phi+\beta_S) \\
&- M_{D1}e_D\ddot{v}\sin(\phi+\beta_D)\,\delta\left(x-\frac{L}{3}\right) \\
&+ M_{D1}e_D\ddot{w}\cos(\phi+\beta_D)\delta\left(x-\frac{L}{3}\right) + I_{PD1}\ddot{\phi}\delta\left(x-\frac{L}{3}\right) \\
&+ I_{PD1}\frac{\partial}{\partial t}(w'\dot{v}')\delta\left(x-\frac{L}{3}\right) + I_{PD2}\ddot{\phi}\delta(x-L) \\
&+ I_{PD2}\frac{\partial}{\partial t}(w'\dot{v}')\delta(x-L) - T\,\delta\left(x-\frac{L}{3}\right)
\end{aligned}
\qquad (20)
$$

4.5. Perturbation application

To better understand the extent of interaction, applying the perturbation series (as shown in **Equation (21)** to **Equation (34)**),

$$v = \varepsilon v_1 + \varepsilon^2 v_2 + \cdots + \varepsilon^n v_n \qquad (21)$$

$$w = \varepsilon w_1 + \varepsilon^2 w_2 + \cdots + \varepsilon^n w_n \qquad (22)$$

$$\phi = \phi_0 + \varepsilon\phi_1 + \varepsilon^2\phi_2 + \cdots + \varepsilon^n\phi_n \qquad (23)$$

$$T = \varepsilon T_1 + \varepsilon^2 T_2 + \cdots + \varepsilon^n T_n \qquad (24)$$

$$e_S = \varepsilon e_{S1} + \varepsilon^2 e_{S2} + \cdots + \varepsilon^n e_{Sn} \qquad (25)$$

$$e_D = \varepsilon e_{D1} + \varepsilon^2 e_{D2} + \cdots + \varepsilon^n e_{Dn} \qquad (26)$$

$$F_{Shaft,y} = \varepsilon F_{Shaft,y1} + \varepsilon^2 F_{Shaft,y2} + \cdots + \varepsilon^n F_{Shaft,yn} \qquad (27)$$

$$F_{Shaft,z} = \varepsilon F_{Shaft,z1} + \varepsilon^2 F_{Shaft,z2} + \cdots + \varepsilon^n F_{Shaft,zn} \qquad (28)$$

$$F_{Disc,y} = \varepsilon F_{Disc,y1} + \varepsilon^2 F_{Disc,y2} + \cdots + \varepsilon^n F_{Disc,yn} \qquad (29)$$

$$F_{Disc,z} = \varepsilon F_{Disc,z1} + \varepsilon^2 F_{Disc,z2} + \cdots + \varepsilon^n F_{Disc,zn} \qquad (30)$$

Similarly, using Taylor's series expansion for harmonic terms,

$$\sin(\phi + \beta_S) = \sin(\phi_0 + \beta_S) + \varepsilon\phi_1 \cos(\phi_0 + \beta_S) + \ldots \quad (31)$$

$$\cos(\phi + \beta_S) = \cos(\phi_0 + \beta_S) - \varepsilon\phi_1 \sin(\phi_0 + \beta_S) + \ldots \quad (32)$$

$$\sin(\phi + \beta_D) = \sin(\phi_0 + \beta_D) + \varepsilon\phi_1 \cos(\phi_0 + \beta_D) + \ldots \quad (33)$$

$$\cos(\phi + \beta_D) = \cos(\phi_0 + \beta_D) - \varepsilon\phi_1 \sin(\phi_0 + \beta_D) + \ldots \quad (34)$$

4.6. Equation of motion of different orders

4.6.1. First order

At the $O(\varepsilon)$, the obtained equation of motion in three fundamental directions is as shown in **Equation (35)**, **Equation (36)**, and **Equation (37)**.

$$\begin{aligned} m\ddot{v}_1 + EIv_1{}'''' - I_{PS}(\Omega\dot{w}_1{}')' - I_{DS}\ddot{v}_1{}'' \\ = \frac{\partial}{\partial t}(me_{S1}\Omega\sin(\phi_o + \beta_S)) - M_{D1}\ddot{v}_1\delta\left(x - \frac{L}{3}\right) \\ + \frac{\partial}{\partial t}(M_{D1}e_{D1}\Omega\sin(\phi_o + \beta_D))\,\delta\left(x - \frac{L}{3}\right) + I_{PD1}(\Omega\dot{w}_1{}')'\delta\left(x - \frac{L}{3}\right) \\ + I_{DD1}\ddot{v}_1{}''\delta\left(x - \frac{L}{3}\right) - M_{D2}\ddot{v}_1\delta(x - L) + I_{PD2}(\Omega\dot{w}_1{}')'\delta(x - L) \\ + I_{DD2}\ddot{v}_1{}''\delta(x - L) + F_{Shaft,y1} + F_{Disc,y1}\delta\left(x - \frac{L}{3}\right) \end{aligned} \quad (35)$$

$$\begin{aligned} m\ddot{w}_1 + EIw_1{}'''' + I_{PS}(\Omega\dot{v}_1{}')' - I_{DS}\ddot{w}_1{}'' \\ = -\frac{\partial}{\partial t}(me_{S1}\Omega\cos(\phi_o + \beta_S)) - M_{D1}\ddot{w}_1\delta\left(x - \frac{L}{3}\right) \\ - \frac{\partial}{\partial t}(M_{D1}e_{D1}\Omega\cos(\phi_o + \beta_D))\delta\left(x - \frac{L}{3}\right) - I_{PD1}(\Omega\dot{v}_1{}')'\delta\left(x - \frac{L}{3}\right) \\ + I_{DD1}\ddot{w}_1{}''\delta\left(x - \frac{L}{3}\right) - M_{D2}\ddot{w}_1\delta(x - L) - I_{PD2}(\Omega\dot{v}_1{}')'\delta(x - L) \\ + I_{DD2}\ddot{w}_1{}''\delta(x - L) + F_{Shaft,z1} + F_{Disc,z1}\delta\left(x - \frac{L}{3}\right) \end{aligned} \quad (36)$$

$$GJ\phi_1{}'' - I_{PS}\ddot{\phi}_1 = I_{PD1}\ddot{\phi}_1\,\delta\left(x - \frac{L}{3}\right) + I_{PD2}\ddot{\phi}_1\,\delta(x - L) - T_1\delta\left(x - \frac{L}{3}\right) \quad (37)$$

The absence of torsional vibration component in the transverse vibration equation, and the absence of transverse vibration term in the torsional vibration equation, demonstrates the complete decoupling of the transverse and torsional terms in the case for first order.

4.6.2. Second order

At the $O(\varepsilon^2)$, the obtained equation of motion in three fundamental directions is as shown in **Equation (38)**, **Equation (39)** and **Equation (40)**).

$$
\begin{aligned}
&m\ddot{v}_2 + EIv_2{}'''' - I_{PS}\left(\ddot{\phi}_1 w_1{}'\right)' - I_{PS}(\Omega \dot{w}_2{}')' - I_{PS}\left(\dot{\phi}_1 \dot{w}_1{}'\right)' - I_{Ds}\ddot{v}_2{}'' \\
&\quad = \frac{\partial}{\partial t}(me_{S1}\Omega\phi_1 \cos(\phi_o + \beta_S)) + \frac{\partial}{\partial t}(me_{S1}\dot{\phi}_1 \sin(\phi_o + \beta_S)) \\
&\quad + \frac{\partial}{\partial t}(me_{S2}\Omega \sin(\phi_o + \beta_S)) - M_{D1}\ddot{v}_2\delta\left(x - \frac{L}{3}\right) \\
&\quad + \frac{\partial}{\partial t}(M_{D1}e_{D1}\Omega\phi_1 \cos(\phi_o + \beta_D))\delta\left(x - \frac{L}{3}\right) \\
&\quad + \frac{\partial}{\partial t}(M_{D1}e_{D1}\dot{\phi}_1 \sin(\phi_o + \beta_D))\,\delta\left(x - \frac{L}{3}\right) \\
&\quad + \frac{\partial}{\partial t}(M_{D1}e_{D1}\Omega \sin(\phi_o + \beta_D))\delta\left(x - \frac{L}{3}\right) + I_{PD1}\left(\ddot{\phi}_1 w_1{}'\right)'\delta\left(x - \frac{L}{3}\right) \\
&\quad + I_{PD1}(\Omega \dot{w}_2{}')'\delta\left(x - \frac{L}{3}\right) + I_{PD1}\left(\dot{\phi}_1 \dot{w}_1{}'\right)'\delta\left(x - \frac{L}{3}\right) \\
&\quad + I_{DD1}\ddot{v}_2{}''\delta\left(x - \frac{L}{3}\right) - M_{D2}\ddot{v}_2\delta(x - L) + I_{PD2}\left(\ddot{\phi}_1 w_1{}'\right)'\delta(x - L) \\
&\quad + I_{PD2}(\Omega \dot{w}_2{}')'\delta(x - L) + I_{PD2}\left(\dot{\phi}_1 \dot{w}_1{}'\right)'\delta(x - L) \\
&\quad + I_{DD2}\ddot{v}_2{}''\delta(x - L) - T_1 w_1{}''\delta\left(x - \frac{L}{3}\right) + F_{Shaft,y2} \\
&\quad + F_{Disc,y2}\delta\left(x - \frac{L}{3}\right)
\end{aligned}
\tag{38}
$$

$$
\begin{aligned}
&m\ddot{w}_2 + EIw_2{}'''' + I_{PS}(\Omega \dot{v}_2{}')' + I_{PS}\left(\dot{\phi}_1 \dot{v}_1{}'\right)' - I_{Ds}\ddot{w}_2{}'' \\
&\quad = \frac{\partial}{\partial t}(me_{S1}\Omega\phi_1 \sin(\phi_o + \beta_S)) - \frac{\partial}{\partial t}(me_{S1}\dot{\phi}_1 \cos(\phi_o + \beta_S)) \\
&\quad - \frac{\partial}{\partial t}(me_{S2}\Omega \cos(\phi_o + \beta_S)) - M_{D1}\ddot{w}_2\delta\left(x - \frac{L}{3}\right) \\
&\quad + \frac{\partial}{\partial t}(M_{D1}e_{D1}\Omega\phi_1 \sin(\phi_o + \beta_D))\delta\left(x - \frac{L}{3}\right) \\
&\quad - \frac{\partial}{\partial t}(M_{D1}e_{D1}\dot{\phi}_1 \cos(\phi_o + \beta_D))\,\delta\left(x - \frac{L}{3}\right) \\
&\quad - \frac{\partial}{\partial t}(M_{D1}e_{D2}\Omega \cos(\phi_o + \beta_D))\delta\left(x - \frac{L}{3}\right) - I_{PD1}(\Omega \dot{v}_2{}')'\delta\left(x - \frac{L}{3}\right) \\
&\quad - I_{PD1}\left(\dot{\phi}_1 \dot{v}_1{}'\right)'\delta\left(x - \frac{L}{3}\right) + I_{DD1}\ddot{w}_2{}''\delta\left(x - \frac{L}{3}\right) - M_{D2}\ddot{w}_2\delta(x - L) \\
&\quad - I_{PD2}(\Omega \dot{v}_2{}')'\delta(x - L) - I_{PD2}\left(\dot{\phi}_1 \dot{v}_1{}'\right)'\delta(x - L) + I_{DD2}\ddot{w}_2{}''\delta(x - L) \\
&\quad - T_1 v_1{}''\delta\left(x - \frac{L}{3}\right) + F_{Shaft,z2} + F_{Disc,z2}\delta\left(x - \frac{L}{3}\right)
\end{aligned}
\tag{39}
$$

$$
\begin{aligned}
GJ\phi_2{}'' - I_{PS}\ddot{\phi}_2 - I_{PS}\frac{\partial}{\partial t}(\dot{v}_1{}'w_1{}') \\
&= -me_{S1}\ddot{v}_1\sin(\phi_o+\beta_S) + me_{S1}\ddot{w}_1\cos(\phi_o+\beta_S) \\
&\quad - M_{D1}e_{D1}\ddot{v}_1\sin(\phi_o+\beta_D)\delta\left(x-\frac{L}{3}\right) \\
&\quad + M_{D1}e_{D1}\ddot{w}_1\cos(\phi_o+\beta_D)\delta\left(x-\frac{L}{3}\right) + I_{PD1}\ddot{\phi}_2\delta\left(x-\frac{L}{3}\right) \\
&\quad + I_{PD1}\frac{\partial}{\partial t}(\dot{v}_1{}'w_1{}')\delta\left(x-\frac{L}{3}\right) + I_{PD2}\ddot{\phi}_2\delta(x-L) \\
&\quad + I_{PD2}\frac{\partial}{\partial t}(\dot{v}_1{}'w_1{}')\delta(x-L) - T_2\delta\left(x-\frac{L}{3}\right)
\end{aligned}
\qquad (40)
$$

It is observed that the terms of transverse vibration appears in the equation of motion of torsional vibration as a forcing term, and torsional vibration appears in the equation of motion of transverse vibration as a forcing term.

CHAPTER FIVE: ANALYTICAL SOLUTION

To better understand the extent of interaction, the system is made to operate at constant angular speed Ω. Furthermore, for simplicity, it is assumed that there exists no fluctuation in torque as well as force.

Based on these assumptions, the analytical solution in this study is developed for the torsional vibration of the system.

5.1. First order

To solve the equation of motion of first-order torsional vibration, using the assumed mode method, the torsional response can be expressed as shown in **Equation (41)**,

$$\phi_1(x,t) = \sum_{n=1}^{\infty} \phi_n(t) \sin\left(\frac{n\pi x}{2L}\right) \tag{41}$$

Similarly, the temporal and spatial derivatives (Second order) of **Equation (41)** are given as shown in **Equation (42)** and **Equation (43)**, respectively.

$$\ddot{\phi_1}(x,t) = \sum_{n=1}^{\infty} \ddot{\phi_n}(t) \sin\left(\frac{n\pi x}{2L}\right) \tag{42}$$

$$\phi_1{}''(x,t) = -\sum_{n=1}^{\infty} \phi_n(t) \left(\frac{n\pi}{2L}\right)^2 \sin\left(\frac{n\pi x}{2L}\right) \tag{43}$$

Substituting **Equation (42)** and **Equation (43)** in **Equation (37)**, we get

$$\begin{aligned} -GJ \sum_{n=1}^{\infty} \phi_n(t) \left(\frac{n\pi}{2L}\right)^2 \sin\left(\frac{n\pi x}{2L}\right) - I_{PS} \sum_{n=1}^{\infty} \ddot{\phi_n}(t) \sin\left(\frac{n\pi x}{2L}\right) \\ - I_{PD1} \sum_{n=1}^{\infty} \ddot{\phi_n}(t) \sin\left(\frac{n\pi x}{2L}\right) \delta\left(x - \frac{L}{3}\right) \\ - I_{PD2} \sum_{n=1}^{\infty} \ddot{\phi_n}(t) \sin\left(\frac{n\pi x}{2L}\right) \delta(x - L) = 0 \end{aligned} \tag{44}$$

Using conditions of orthogonality, after application of the assumed mode method in **Equation (44)**, the equation of Torsional vibration reduces to an ODE as shown in **Equation (45)**,

$$\left[GJ \left(\frac{n\pi}{2L}\right)^2 \left(\frac{L}{2}\right)\right] \ddot{\phi_n}(t) + \left[I_{PS}\left(\frac{L}{2}\right) + I_{PD1} \sin^2\left(\frac{n\pi}{6L}\right) + \frac{I_{PD2}}{2} \sin^2\left(\frac{n\pi}{2L}\right)\right] \phi_n(t) = 0 \tag{45}$$

From **Equation (45),** it can be clearly seen that the torsional natural frequency for n^{th} mode is given as shown in **Equation (46)**.

$$\delta_n = \sqrt{\frac{GJ\left(\frac{n\pi}{2L}\right)^2\left(\frac{L}{2}\right)}{I_{PS}\left(\frac{L}{2}\right) + I_{PD1}\sin^2\left(\frac{n\pi}{6L}\right) + \frac{I_{PD2}}{2}\sin^2\left(\frac{n\pi}{2L}\right)}} \tag{46}$$

5.2. Second order

To solve the equation of motion of $O(\varepsilon^2)$, the transverse displacements can be expressed as shown in **Equation (47)** and **Equation (48),** respectively.

$$v_1(x,t) = \sum_{n=1}^{\infty} X_n(x)\ \cos(\Omega t + \beta) \tag{47}$$

$$w_1(x,t) = \sum_{n=1}^{\infty} X_n(x)\ \sin(\Omega t + \beta) \tag{48}$$

The term $X_n(x)$ in **Equation (47)** and **Equation (48)** can be expressed in piecewise form as shown in **Equation (49)**.

$$X_n(x) = \begin{cases} X_1(x), & 0 \le x \le \frac{L}{3} \\ X_2(x), & \frac{L}{3} \le x \le \frac{2L}{3} \\ X_3(x), & \frac{2L}{3} \le x \le L \end{cases} \tag{49}$$

Equation (49) can be further expressed in transcendental form as shown below in **Equation (50)**, **Equation (51)**, and **Equation (52)**.

$$X_1(x) = a\sin(\beta x) + b\cos(\beta x) + c\sinh(\beta x) + d\cosh(\beta x) \tag{50}$$

$$X_2(x) = e\sin(\beta x) + f\cos(\beta x) + g\sinh(\beta x) + h\cosh(\beta x) \tag{51}$$

$$X_3(x) = i\sin(\beta x) + j\cos(\beta x) + k\sinh(\beta x) + l\cosh(\beta x) \tag{52}$$

To solve the above mentioned sets of equation, the boundary condition are set as follows.

At the left bearing, deflection and moment are equal to zero.

$$X_1(0) = 0 \tag{53}$$

$$\frac{d^2X_1(0)}{dx^2} = 0 \tag{54}$$

At the point of application of First disc in between the bearings, there exists continuity in deflection, slope, and moment values, followed by a jump in shear force.

$$X_1\left(\frac{L}{3}\right) - X_2\left(\frac{L}{3}\right) = 0 \tag{55}$$

$$\frac{dX_1\left(\frac{L}{3}\right)}{dx} - \frac{dX_2\left(\frac{L}{3}\right)}{dx} = 0 \tag{56}$$

$$\frac{d^2X_1\left(\frac{L}{3}\right)}{dx^2} - \frac{d^2X_2\left(\frac{L}{3}\right)}{dx^2} = 0 \tag{57}$$

$$\frac{d^3X_2\left(\frac{L}{3}\right)}{dx^3} - \frac{d^3X_1\left(\frac{L}{3}\right)}{dx^3} - \frac{m_1\beta^4}{\rho A}X_1\left(\frac{L}{3}\right) = 0 \tag{58}$$

Similarly, at the right bearing deflection is zero, followed by continuity in values of slope and moment.

$$X_2\left(\frac{2L}{3}\right) = 0 \tag{59}$$

$$X_3\left(\frac{2L}{3}\right) = 0 \tag{60}$$

$$\frac{dX_2\left(\frac{2L}{3}\right)}{dx} - \frac{dX_3\left(\frac{2L}{3}\right)}{dx} = 0 \tag{61}$$

$$\frac{d^2X_2\left(\frac{2L}{3}\right)}{dx^2} - \frac{d^2X_3\left(\frac{2L}{3}\right)}{dx^2} = 0 \tag{62}$$

Similarly, at the free end moment value is zero, followed by a jump in shear force values.

$$\frac{d^2X_3(L)}{dx^2} = 0 \tag{63}$$

$$\frac{d^3X_3(L)}{dx^3} - \frac{m_2\beta^4}{\rho A}X_3(L) = 0 \qquad (64)$$

The above-mentioned set of equations from **Equation (53)** to **Equation (64),** when substituted in **Equation (50)**, **Equation (51)**, and **Equation (52),** gives the required transcendental equation.

Substituting **Equation (47)** and **Equation (48)** in **Equation (40),** we get,

$$\begin{aligned} -GJ\sum_{n=1}^{\infty}\phi_n(t)\left(\frac{n\pi}{2L}\right)^2\sin\left(\frac{n\pi x}{2L}\right) - I_{PS}\sum_{n=1}^{\infty}\ddot{\phi_n}(t)\sin\left(\frac{n\pi x}{2L}\right) \\ - I_{PD1}\sum_{n=1}^{\infty}\ddot{\phi_n}(t)\sin\left(\frac{n\pi x}{2L}\right)\delta\left(x-\frac{L}{3}\right) \\ - I_{PD2}\sum_{n=1}^{\infty}\ddot{\phi_n}(t)\sin\left(\frac{n\pi x}{2L}\right)\delta(x-L) \\ = I_{PS}\frac{\partial}{\partial t}(\dot{v_1}'w_1') + I_{PD1}\frac{\partial}{\partial t}(\dot{v_1}'w_1')\delta\left(x-\frac{L}{3}\right) \\ + I_{PD2}\frac{\partial}{\partial t}(\dot{v_1}'w_1')\delta(x-L) \end{aligned} \qquad (65)$$

Although the torsional mode shape function theoretically spans from $n = 1$ to $n = \infty$, for simplicity and to reduce computational effort, only the fundamental mode (First mode) corresponding to $n = 1$ is considered in this analysis.

Using conditions of orthogonality, after application of the assumed mode method in **Equation (65)**, the equation of Torsional vibration reduces to,

$$\ddot{\phi}(t) + {\delta_1}^2\phi(t) = \frac{1}{I_{PS}\left(\frac{L}{2}\right) + I_{PD1}\sin^2\left(\frac{\pi}{6L}\right) + \frac{I_{PD2}}{2}\sin^2\left(\frac{\pi}{2L}\right)}\Omega^2F_r\sin 2(\Omega t+\beta) \qquad (66)$$

The term F_r in **Equation (66)** is given as shown in **Equation (67)**.

$$\begin{aligned} F_r = \frac{1}{\Omega^2\sin[2(\Omega t+\beta)]}\Bigg[\int_0^L\Bigg(I_{PS}\frac{\partial}{\partial t}(\dot{v_1}'w_1') + I_{PD1}\frac{\partial}{\partial t}(\dot{v_1}'w_1')\delta\left(x-\frac{L}{3}\right) \\ + I_{PD2}\frac{\partial}{\partial t}(\dot{v_1}'w_1')\delta(x-L)\Bigg)\Bigg]\sin\left(\frac{\pi x}{2L}\right)dx \end{aligned} \qquad (67)$$

The value of Term F_r can be solved computationally, and can be used in further analysis for determination of the final coupled torsional response.

It is clearly evident that **Equation (66)** resembles that of the SDOF harmonic oscillator, and it is obvious to assume the solution as,

$$\phi(t) = \phi_r \sin 2(\Omega t + \beta) \tag{68}$$

Substituting **Equation (68)** in **Equation (66)** we get,

$$\phi_r = \frac{1}{I_{PS}\left(\frac{L}{2}\right) + I_{PD1}\sin^2\left(\frac{\pi}{6L}\right) + \frac{I_{PD2}}{2}\sin^2\left(\frac{\pi}{2L}\right)} \frac{F_r}{4}\left(\frac{1}{-1 + \left(\frac{\delta}{2\Omega}\right)^2}\right) \tag{69}$$

Substituting **Equation (69)** in **Equation (68)**, the temporal response reduces as shown in **Equation (70)**.

$$\phi(t) = \frac{1}{I_{PS}\left(\frac{L}{2}\right) + I_{PD1}\sin^2\left(\frac{\pi}{6L}\right) + \frac{I_{PD2}}{2}\sin^2\left(\frac{\pi}{2L}\right)} \frac{F_r}{4}\left(\frac{1}{-1 + \left(\frac{\delta}{2\Omega}\right)^2}\right) \sin 2(\Omega t + \beta) \tag{70}$$

Substituting **Equation (70)** in **Equation (41),** the combined Spatial as well as temporal response (Considering only the Fundamental mode) reduces as shown in **Equation (71)**.

$$\phi(x,t) = \frac{1}{I_{PS}\left(\frac{L}{2}\right) + I_{PD1}\sin^2\left(\frac{\pi}{6L}\right) + \frac{I_{PD2}}{2}\sin^2\left(\frac{\pi}{2L}\right)} \frac{F_r}{4}\left(\frac{1}{-1 + \left(\frac{\delta}{2\Omega}\right)^2}\right) \sin 2(\Omega t + \beta) \sin\left(\frac{\pi x}{2L}\right) \tag{71}$$

It is evident that the flexural motion is responsible for torsional motion at twice the spin speed. Therefore, resonance may occur when the spin speed (Ω) is close to one-half of any of the torsional natural frequencies (δ).

CHAPTER SIX: NUMERICAL EXAMPLE IMPLEMENTATION

6.1. Analytical numerical solution

For a numerical example implementation, the following tabulated parameters are taken as shown in **Table 1**. Further, the system is made to operate at a constant rotational speed of 1500 RPM to observe the torsional response.

Table 1: *System parameters.*

S.N.	Parameters	Values
1	Mass of First Disc	2575 kg
2	Diameter of First Disc	176 cm
3	Moment of inertia of the First Disc about the transverse axis	499 kg·m²
4	Polar moment of inertia of the First Disc about the longitudinal axis	998 kg·m²
5	Mass of Second Disc	35000 kg
6	Diameter of Second Disc	240 cm
7	Moment of inertia of the Second Disc about the transverse axis	12600 kg·m²
8	Polar moment of inertia of the Second Disc about the longitudinal axis	25200 kg·m²
9	Density of the shaft	7850 kg/m³
10	Diameter of the shaft	50 cm
11	Young's modulus of elasticity of the shaft material	202 GPa
12	Shaft cross-sectional area, moment of inertia about the transverse axis	0.003067 m⁴
13	Shaft cross-sectional polar area moment of inertia about the longitudinal axis	0.006135 m⁴
14	Cross-sectional area of the shaft	0.1963 m²
15	Length of the shaft	100 cm

6.1.1. First order

Substituting the tabulated parameters as shown in **Table 1**, the fundamental mode torsional natural frequency (δ) (From **Equation (46)**) is obtained as 35.38 Hz.

6.1.2. Second order

Using the tabulated parameters as shown in **Table 1**, the bending vibration mode shapes are given as shown in **Equation (72)**, **Equation (73)**, and **Equation (74)**.

$$X_1(x) = \begin{cases} sin(1.041576829x) - 0.8520812506sinh(1.041576829x), & x \le \frac{1}{3} \\ 0.9685404103\sin(1.041576829x) \\ +\ 0.01138364949\cos(1.041576829x) \\ -\ 0.8165886482sinh(1.041576829x) - 0.01185038236cosh(1.041576829x), & \frac{1}{3} \le x \le \frac{2}{3} \\ -1.104606707\sin(1.041576829x) + 1.737764042\cos(1.041576829x) \\ +\ 2.558214724sinh(1.041576829x) - 2.039402990cosh(1.041576829x), & x \ge \frac{2}{3} \end{cases} \quad (72)$$

$$X_2(x) = \begin{cases} sin(3.385526128x) - 0.3029701293sinh(3.385526128x), & x \le \frac{1}{3} \\ 0.4133741012sin(3.385526128x) \\ +1.238709734cos(3.385526128x) \\ -\ 2.037019144sinh(3.385526128x) - 1.896580619cosh(3.385526128x), & \frac{1}{3} \le x \le \frac{2}{3} \\ -0.5032041477sin(3.385526128x) + 0.1195704087cos(3.385526128x) \\ -\ 4.949383429sinh(3.385526128x) + 4.938419919cosh(3.385526128x), & x \ge \frac{2}{3} \end{cases} \quad (73)$$

$$X_3(x) = \begin{cases} sin(9.427102050x) + 0.00005182028418sinh(9.427102050x), & x \le \frac{1}{3} \\ 0.9986155264sin(9.427102050x) \\ +1.072503588\,.10^{-6}cos(9.427102050x) \\ -0.01600932793sinh(9.427102050x) + 0.01600136600cosh(9.427102050x), & \frac{1}{3} \le x \le \frac{2}{3} \\ 0.9945380776sin(9.427102050x) + +7.381385044.10^{-6}\ cos(9.427102050\ x) \\ +1.077431180\ sinh(9.427102050\ x) - 1.077431539cosh(9.427102050x), & x \ge \frac{2}{3} \end{cases} \quad (74)$$

The corresponding mode shapes for three different modes are shown in **Figure 4**.

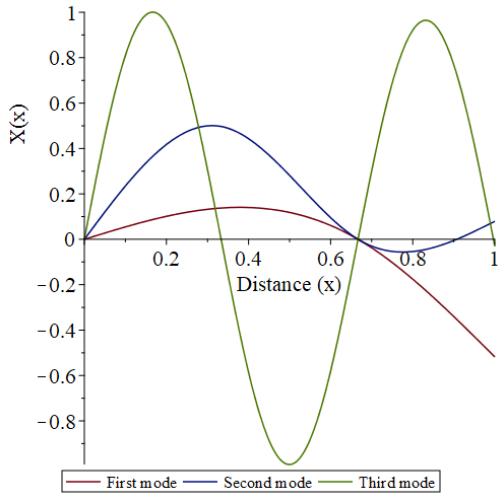

Figure 4: *Mode shapes obtained through analytical solution.*

Substituting **Equation (72)**, **Equation (73)**, and **Equation (74)** in **Equation (49)** and thereafter into **Equation (47)** and **Equation (48)**, **Equation (67)** can be solved computationally to obtain the value of F_r as 1384.86.

The value of F_r and δ, along with tabulated parameters as shown in **Table 1** when substituted in **Equation (71)** leads to the development of the final torsional response as shown in **Equation (75)**.

$$\phi(x,t) = 0.054 \sin\left(\frac{\pi x}{2}\right) \sin(314.20t) \qquad (75)$$

Equation (75) gives the response of the system in radians. **Equation (75),** when plotted in the spatial as well as temporal domain, gives the final torsional response of the system as shown in **Figure 5**.

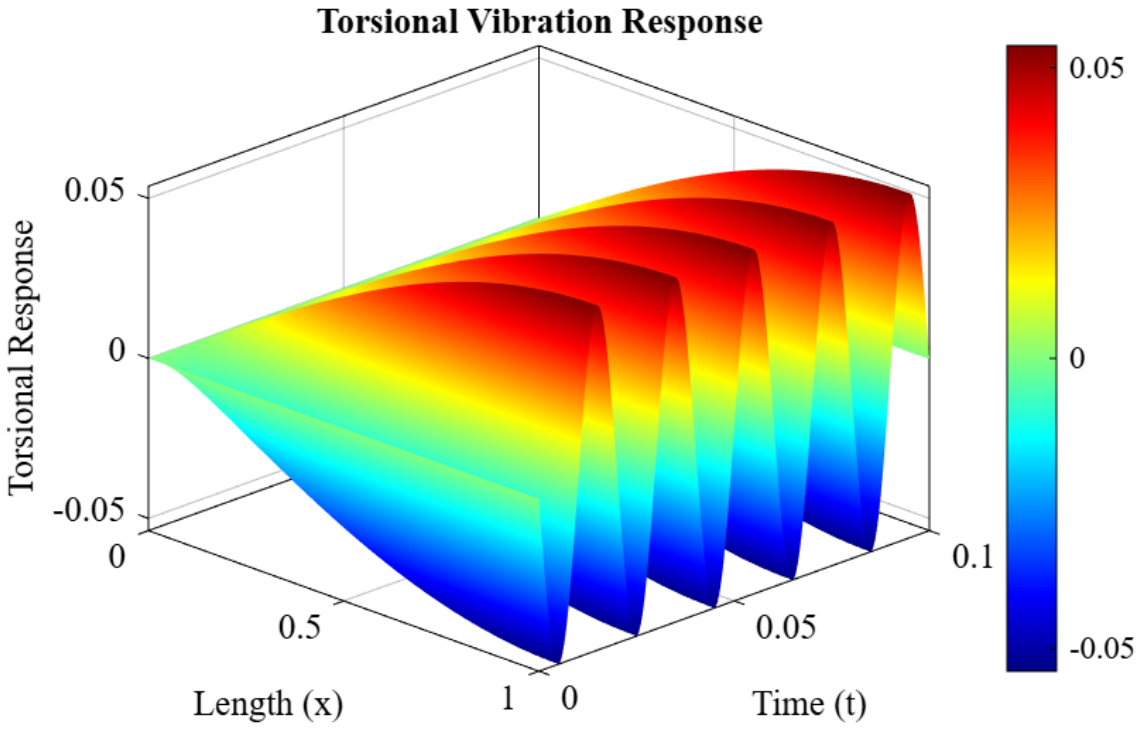

Figure 5: *Torsional vibration response in spatial as well as temporal domain.*

Figure 5 clearly shows that the response of the system is sinusoidal in the spatial as well as the temporal domain.

6.2. Simulation-based solution

Finite element analysis was used to implement the simulation-based solution. For the model, a three-dimensional tetrahedral mesh with a consistent element size of 25 mm was created. In order to better reflect the real support condition, the right bearing was constrained against translation but permitted rotational freedom, while the left bearing was constrained to restrict both translational and rotational degrees of freedom through remote displacements at the bearing locations.

Two lumped masses were included at the proper locations (at $x = \frac{L}{3}$ and at $x = L$) to represent the discs in order to appropriately model the physical system. The shaft was then excited, and its torsional response was obtained by applying a torsional moment to the system.

The simulation-based solution produced the corresponding values at the location of discs, as shown in **Table 2** as well as in **Figure 6** and **Figure 7**, respectively.

Table 2: *Comparative results between analytical and simulation results.*

Method	**At $x = \frac{L}{3}$**	**At $x = L$**
Analytical	6.726 mm (0.027 rad)	13.453 mm (0.054 rad)
Simulation	6.985 mm (0.028 rad)	14.571 mm (0.058 rad)

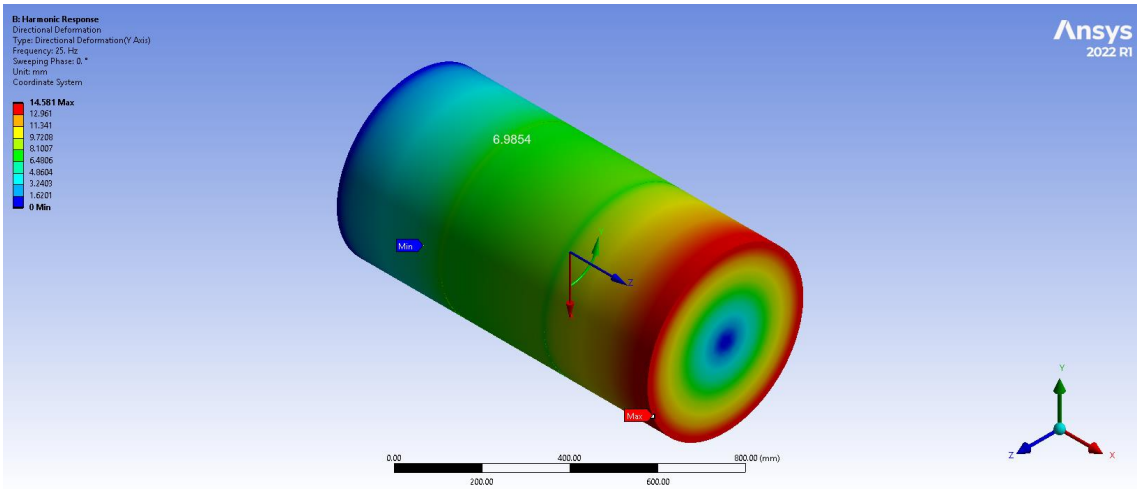

Figure 6: *Torsional vibration response at* $x = L/3$

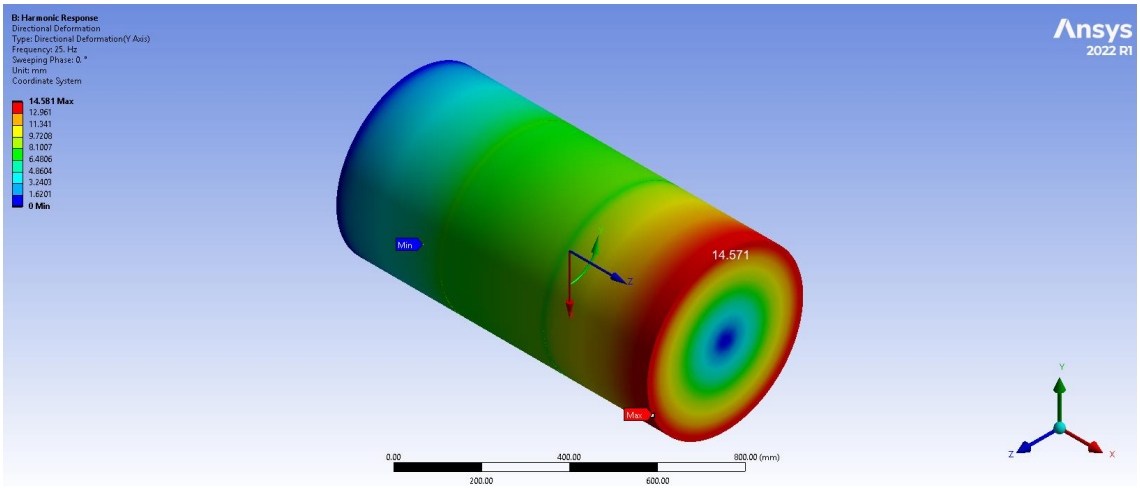

Figure 7: *Torsional vibration response at* $x = L$.

CHAPTER SEVEN: CONCLUSION AND RECOMMENDATIONS

7.1. Conclusion

a) The governing differential equation of motion for the Euler-Bernoulli beam is developed using Extended Hamilton's principle, and the system of equations obtained is found to be a coupled system of partial differential equations.

b) The use of perturbation series allowed the equation of motion to be hierarchically separated into different orders to study the extent of interaction, which showed that coupling occurs in the second and higher orders.

c) The transcendental mode shape function for a pinned-pinned overhung beam with a lumped mass at the free end and an intermediate lumped mass is formulated in a piecewise manner.

d) The assumed mode method is employed to solve the equation of motion for torsional response, which reveals that the flexural motion of frequency $\boldsymbol{\Omega}$ excites torsional motion at twice that frequency, and resonance can take place if the operational speed approaches close to half of the torsional natural frequency.

e) Numerical example is implemented to the obtained solutions, which yielded closely matching results in between the analytical and simulation approaches. At $x = \frac{L}{3}$, the analytical values are 6.726 mm (0.027 rad) compared to 6.985 mm (0.028 rad) from simulation, while at $x = L$, the analytical results are 13.453 mm (0.054 rad) and the simulation produced 14.571 mm (0.058 rad).

7.2. Recommendations

This work can be further extended as following:

a) The beam can be modelled as a Timoshenko beam, to incorporate the effects of shear deformation and rotary inertia, leading to a more accurate representation of system dynamics.

b) The present study can be further extended by considering the disc as a flexible element instead of rigid bodies to better incorporate the deformation effects on the entire system dynamics.

c) The assumption of rigid bearings can be modified by the use of flexible damped bearings, which would more realistically represent the conditions of support.

d) Inclusion of higher modes, beyond the fundamental mode, can help achieve more comprehensive results of torsional response.

e) The model can be further improved in simulation part by accounting the distributed eccentricity along the length of shaft.

REFERENCES

Al-Bedoor, B. O. (1999). Dynamic model of coupled shaft torsional and blade bending deformations in rotors. *Computer Methods in Applied Mechanics and Engineering*, *169*(1–2), 177–190. https://doi.org/10.1016/S0045-7825(98)00184-4

Al-Bedoor, B. O. (2000). Transient torsional and lateral vibrations of unbalanced rotors with rotor-to-stator rubbing. *Journal of Sound and Vibration*, *229*(3), 627–645. https://doi.org/10.1006/jsvi.1999.2513

Al-Bedoor, B. O. (2001). Modeling the coupled torsional and lateral vibrations of unbalanced rotors. *Computer Methods in Applied Mechanics and Engineering*, *190*(45), 5999–6008. https://doi.org/10.1016/S0045-7825(01)00209-2

Al-Bedoor, B. O., & Al-Qaisia, A. A. (2005). Stability analysis of rotating blade bending vibration due to torsional excitation. *Journal of Sound and Vibration*, *282*(3–5), 1065–1083. https://doi.org/10.1016/j.jsv.2004.03.038

Bernasconi, O. (1987). Bisynchronous Torsional Vibrations in Rotating Shafts. *Journal of Applied Mechanics*, *54*(4), 893–897. https://doi.org/10.1115/1.3173135

Broniarek, C. (1968). Investigation of the coupled flexural-torsional vibrations of rotors with continuous parameters (Bending vibratory motion instability of rotor on elastic shaft with uniform mass distribution along axis, using variational methods). *ZAGADNIENIA DRGAN NIELINIOWYCH*, (9), 169–228.

Cohen, R., & Porat, I. (1985). Coupled torsional and transverse vibration of unbalanced rotor. *Journal of Applied Mechanics*, *52*, 701–705.

Dahal, S., Shakya, P. R., Kandel, M., & Luintel, M. C. (2023). Coupled Torsional And Transverse Vibration Analysis Of Double Overhung Rotor Shaft Centrifugal Fan. *14th IOE Graduate Conference*.

Darpe, A. K., Gupta, K., & Chawla, A. (2004). Coupled bending, longitudinal and torsional vibrations of a cracked rotor. *Journal of Sound and Vibration*, *269*(1–2), 33–60. https://doi.org/10.1016/S0022-460X(03)00003-8

Gasch, R., Markert, R., & Pfützner, H. (1979). Acceleration of unbalanced flexible rotors through the critical speeds. *Journal of Sound and Vibration*, *63*(3), 393–409.

Kellenberger, W. (1980). Resonances combinees' forcees de l'arbre tournant. Couplage de flexion et de torsion (Pt. 117-121). *Revue Brown Bovery*, *2–80*.

Mohiuddin, M. A., & Khulief, Y. A. (1999). Coupled bending torsional vibration of rotors using finite element. *Journal of Sound and Vibration*, *223*(2), 297–316. https://doi.org/10.1006/jsvi.1998.2095

Nataraj, C. (1993). On the Interaction of Torsion and Bending in Rotating Shafts. *Journal of Applied Mechanics*, *60*(1), 239–241. https://doi.org/10.1115/1.2900762

Perera, I. (1998). *Theoretical and experimental study of coupled torsional-lateral vibrations in rotor dynamics*.

Poudel, S., & Luintel, M. C. (2022). Coupled Lateral and Torsional Vibration of a Rigid Disk Attached to a Flexible Shaft. *12th IOE Graduate Conference*, 1634–1641.

Tondl, A. (1965). *Some Problems of Rotor Dynamics*. Publishing House of the Czechoslovak Academy of Sciences.

Zheng-ce, S., Jian-xue, X., Tong, Z., & Ning, T. (2003). Study on influence of bending-torsion coupling in an impacting-rub rotor system. *Applied Mathematics and Mechanics*, *24*(11), 1316–1323.

Gmail Search mail

Compose

Inbox 655
Starred
Snoozed
Sent
Drafts 24
Purchases
More

Labels

Upgrade

26 of 1,801

[JIEE] Editor Decision

Inbox ×

Thapathali Campus Journal <journal@tcioe.edu.np> 5 Apr 2026, 17:14
to me, mcluintel@ioe.edu.np

Dear Author(s),

We have reached a decision regarding your submission to the Journal of Innovations in Engineering Education, "Development of Transcendental Mode Shape Functions of a Pinned–Pinned Overhung Beam with a Lumped Mass at the Free Overhung and an Intermediate Lumped Mass".

Our decision is to: Accept the Submission

–

With Regards,
Raj Kumar Chaulagain, PhD
Editor-in-Chief
Journal of Innovations in Engineering Education (JIEE)
Institute of Engineering, Thapathali Campus
Kathmandu, Nepal

Reply Reply to all Forward

080MSMDE007 Final Report.pdf

Tribhuvan University

Document Details

Submission ID
trn:oid:::3117:586416938

Submission Date
May 5, 2026, 7:06 PM GMT+5:45

Download Date
May 5, 2026, 7:09 PM GMT+5:45

File Name
080MSMDE007 Final Report.pdf

File Size
1.2 MB

54 Pages

10,380 Words

51,678 Characters

12% Overall Similarity

The combined total of all matches, including overlapping sources, for each database.

Filtered from the Report

- Bibliography
- Quoted Text
- Cited Text
- Small Matches (less than 8 words)
- Methods and Materials

Custom Section Exclusions

{titlesCount} Section Titles, {keywordsCount} Keywords

Section title	No. of Section Starters	Section Starters			
"Acknowledgements"	4	Acknowledgements	Acknowledgement	Acknowledgment	Acknowledgments

Match Groups

- 86 Not Cited or Quoted 12%
  Matches with neither in-text citation nor quotation marks
- 0 Missing Quotations 0%
  Matches that are still very similar to source material
- 0 Missing Citation 0%
  Matches that have quotation marks, but no in-text citation
- 0 Cited and Quoted 0%
  Matches with in-text citation present, but no quotation marks

Top Sources

11% Internet sources
8% Publications
0% Submitted works (Student Papers)

Integrity Flags

2 Integrity Flags for Review

- Replaced Characters
  167 suspect characters on 8 pages
  Letters are swapped with similar characters from another alphabet.
- Hidden Text
  28 suspect characters on 9 pages
  Text is altered to blend into the white background of the document.

Our system's algorithms look deeply at a document for any inconsistencies that would set it apart from a normal submission. If we notice something strange, we flag it for you to review.

A Flag is not necessarily an indicator of a problem. However, we'd recommend you focus your attention there for further review.

Match Groups

- 86 Not Cited or Quoted 12%
  Matches with neither in-text citation nor quotation marks
- 0 Missing Quotations 0%
  Matches that are still very similar to source material
- 0 Missing Citation 0%
  Matches that have quotation marks, but no in-text citation
- 0 Cited and Quoted 0%
  Matches with in-text citation present, but no quotation marks

Top Sources

11% Internet sources
8% Publications
0% Submitted works (Student Papers)

Top Sources

The sources with the highest number of matches within the submission. Overlapping sources will not be displayed.

1	Internet elibrary.tucl.edu.np	4%
2	Internet conference.ioe.edu.np	2%
3	Internet jaxa.repo.nii.ac.jp	<1%
4	Publication Carlos Yesid Mendivelso-Duarte, Nelson Arzola de la Peña, Wilmer Cruz-Guayacun...	<1%
5	Internet ebin.pub	<1%
6	Internet www.coursehero.com	<1%
7	Internet theses.gla.ac.uk	<1%
8	Internet prism.ucalgary.ca	<1%
9	Internet aura.abdn.ac.uk	<1%
10	Internet theses.ucalgary.ca	<1%

11	Internet saam.africa	<1%
12	Publication Hassan Afshari, Keivan Torabi, Adel Jafarzadeh Jazi. "Exact closed form solution fo...	<1%
13	Internet vdoc.pub	<1%
14	Internet koreascience.or.kr	<1%
15	Publication C. Nataraj. "On the Interaction of Torsion and Bending in Rotating Shafts", Journa...	<1%
16	Internet www.calculatoratoz.com	<1%
17	Publication Hassan, Motaz M.. "A Novel On-Orbit Reusable Adhesive for an Autonomous Mobi...	<1%
18	Internet pure.kfupm.edu.sa	<1%
19	Internet gyan.iitg.ernet.in	<1%
20	Publication Yuan, Z.. "External and internal coupling effects of rotor's bending and torsional ...	<1%
21	Publication Forral, L.. "Stability Analysis of Symmetrical Rotor-Bearing Systems With Internal ...	<1%
22	Publication Y.C. Tsai, J.M. Hsieh. "An analysis of cutting-edge curves and machining performa...	<1%
23	Publication Yuanhang Hou, Shuqian Cao, Yanhong Kang, Guanwu Li. "Dynamics Analysis of B...	<1%
24	Publication (Agnes) Muszynska, . "Selected Topics on Rotordynamics", Dekker Mechanical En...	<1%

25	Publication Mohammad Rokn-Abadi, Sadegh Amirzadegan, RD Firouzabadi, Mohammad Ali K...	<1%
26	Internet the-eis.com	<1%
27	Publication Aircraft Engineering and Aerospace Technology, Volume 77, Issue 1 (2006-09-19)	<1%
28	Publication Arnab Banerjee, Kamal Krishna Bera. "An Introduction to Waves in Mechanical Pe...	<1%
29	Publication Zahra Bayat, Hassan Haddadpour, Zahra Zamani. "Coupled bending torsional vibr...	<1%
30	Internet apps.dtic.mil	<1%
31	Internet dri.ufu.br	<1%
32	Internet git.cs.tu-dortmund.de	<1%
33	Internet ise.ait.ac.th	<1%
34	Internet media.proquest.com	<1%
35	Publication AL-BEDOOR, B.O.. "TRANSIENT TORSIONAL AND LATERAL VIBRATIONS OF UNBAL...	<1%
36	Publication Manfred Ploechl. "Road and Off-Road Vehicle System Dynamics Handbook", CRC ...	<1%
37	Publication Mechanisms and Machine Science, 2015.	<1%
38	Publication P. Raghavendra Rao, K. Raja Sekhar. "Effects of couple stresses and surface rough...	<1%

39	Publication S. H. Mirtalaie, M. A. Hajabasi. "Nonlinear axial-lateral-torsional free vibrations an...	<1%
40	Publication Wasserman, I.. "Precession of isolated neutron stars -- II. Magnetic fields and typ...	<1%
41	Publication X Y Shen. "Coupled torsional-lateral vibration of the unbalanced rotor system wit...	<1%
42	Internet ir.nctu.edu.tw	<1%
43	Internet www.mechanicaljournals.com	<1%

080MSMDE007 Final Report.pdf

Tribhuvan University

Document Details

Submission ID
trn:oid:::3117:586416938

Submission Date
May 5, 2026, 7:06 PM GMT+5:45

Download Date
May 5, 2026, 7:09 PM GMT+5:45

File Name
080MSMDE007 Final Report.pdf

File Size
1.2 MB

54 Pages

10,380 Words

51,678 Characters

*% detected as AI

AI detection includes the possibility of false positives. Although some text in this submission is likely AI generated, scores below the 20% threshold are not surfaced because they have a higher likelihood of false positives.

Caution: Review required.

It is essential to understand the limitations of AI detection before making decisions about a student's work. We encourage you to learn more about Turnitin's AI detection capabilities before using the tool.

Disclaimer
Our AI writing assessment is designed to help educators identify text that might be prepared by a generative AI tool. Our AI writing assessment may not always be accurate (i.e., our AI models may produce either false positive results or false negative results), so it should not be used as the sole basis for adverse actions against a student. It takes further scrutiny and human judgment in conjunction with an organization's application of its specific academic policies to determine whether any academic misconduct has occurred.

Frequently Asked Questions

How should I interpret Turnitin's AI writing percentage and false positives?
The percentage shown in the AI writing report is the amount of qualifying text within the submission that Turnitin's AI writing detection model determines was either likely AI-generated text from a large-language model or likely AI-generated text that was likely revised using an AI paraphrase tool or word spinner.

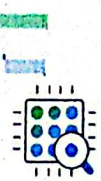

False positives (incorrectly flagging human-written text as AI-generated) are a possibility in AI models.

AI detection scores under 20%, which we do not surface in new reports, have a higher likelihood of false positives. To reduce the likelihood of misinterpretation, no score or highlights are attributed and are indicated with an asterisk in the report (*%).

The AI writing percentage should not be the sole basis to determine whether misconduct has occurred. The reviewer/instructor should use the percentage as a means to start a formative conversation with their student and/or use it to examine the submitted assignment in accordance with their school's policies.

What does 'qualifying text' mean?
Our model only processes qualifying text in the form of long-form writing. Long-form writing means individual sentences contained in paragraphs that make up a longer piece of written work, such as an essay, a dissertation, or an article, etc. Qualifying text that has been determined to be likely AI-generated will be highlighted in cyan in the submission, and likely AI-generated and then likely AI-paraphrased will be highlighted purple.

Non-qualifying text, such as bullet points, annotated bibliographies, etc., will not be processed and can create disparity between the submission highlights and the percentage shown.